

## Matter and singularities

---

David R. Morrison<sup>1,2</sup> and Washington Taylor<sup>3</sup>

<sup>1</sup>*Departments of Mathematics and Physics  
University of California, Santa Barbara  
Santa Barbara, CA 93106, USA*

<sup>2</sup>*Institute for the Physics and Mathematics of the Universe  
University of Tokyo  
Kashiwa, Chiba 277-8582, Japan*

<sup>3</sup>*Center for Theoretical Physics  
Department of Physics  
Massachusetts Institute of Technology  
77 Massachusetts Avenue  
Cambridge, MA 02139, USA*

drm at math.ucsb.edu, wati at mit.edu

ABSTRACT: We analyze the structure of matter representations arising from codimension two singularities in F-theory, focusing on gauge groups  $SU(N)$ . We give a detailed local description of the geometry associated with several types of singularities and the associated matter representations. We also construct global F-theory models for 6D and 4D theories containing these matter representations. The codimension two singularities encountered include examples where the apparent Kodaira singularity type does not need to be completely resolved to produce a smooth Calabi-Yau, examples with rank enhancement by more than one, and examples where the 7-brane configuration is singular. We identify novel phase transitions, in some of which the gauge group remains fixed but the singularity type and associated matter content change along a continuous family of theories. Global analysis of 6D theories on  $\mathbb{P}^2$  with 7-branes wrapped on curves of small degree reproduces the range of 6D supergravity theories identified through anomaly cancellation and other consistency conditions. Analogous 4D models are constructed through global F-theory compactifications on  $\mathbb{P}^3$ , and have a similar pattern of  $SU(N)$  matter content. This leads to a constraint on the matter content of a limited class of 4D supergravity theories containing  $SU(N)$  as a local factor of the gauge group.

---

## Contents

<b>1. Introduction</b>	<b>2</b>
<b>2. Local analysis of codimension two singularities</b>	<b>3</b>
2.1 Standard rank one enhancement: $A_3 \rightarrow D_4$	5
2.2 Incomplete and complete resolutions	7
2.2.1 Enhancement $A_5 \subset D_6$	8
2.2.2 Enhancement $A_5 \subset E_6$	8
2.3 Matter on a singular 7-brane	11
2.3.1 Representation theory and singularities	11
2.3.2 Ordinary double point singularities	14
2.4 Group theory of novel matter representations	17
2.4.1 4-index antisymmetric representation of $SU(8)$	17
2.4.2 Box representation of $SU(4)$	19
<b>3. Systematic analysis of Weierstrass models</b>	<b>19</b>
<b>4. 6D supergravity without tensor fields</b>	<b>30</b>
4.1 $SU(N)$ on curves of degree $b = 1$	30
4.2 $b = 2$	34
4.3 $b = 3$	37
4.4 $b = 4$	38
<b>5. 4D models</b>	<b>39</b>
5.1 4D Weierstrass models	39
5.2 A (mild) constraint on 4D supergravity theories	41
<b>6. Conclusions</b>	<b>42</b>
<b>A. Details of singularity resolutions</b>	<b>43</b>
A.1 Enhancement of $A_3$ on a smooth divisor class	44
A.1.1 Resolution of $A_3$	44
A.1.2 Resolution of local $D_4$ singularity on $s = 0$ slice	45
A.1.3 Enhancement $A_3 \subset D_4$	46
A.2 Enhancement of a local $A_5$ singularity	48
A.2.1 Enhancement $A_5 \subset D_6$	48
A.2.2 Enhancement $A_5 \subset E_6$	50
A.3 Enhancement of $A_3 \rightarrow A_7$ at an ordinary double point	52

## 1. Introduction

Over the last decade, the development of D-branes in string theory has led to dramatic new insights into the connection between gauge theory and geometry. This connection is made particularly explicit in the language of F-theory [1, 2, 3], where gauge theory coupled to supergravity in an even number of space-time dimensions is described by an elliptically fibered Calabi-Yau manifold over a base  $B$  of complex dimension  $d$  for a low-energy theory in  $10 - 2d$  space-time dimensions. Recent reviews of the aspects of F-theory relevant for the discussion in this paper are given in [4, 5].

In F-theory, the structure of the gauge group in the low-energy theory is primarily encoded in the singularities of the elliptic fibration (with certain global aspects of the gauge group encoded in the Mordell–Weil and Tate–Shafarevich groups of the elliptic fibration [6, 7]). In the language of type IIB string theory, the gauge group is carried by 7-branes wrapped on topologically nontrivial cycles (divisors) of the F-theory base manifold  $B$ . In the geometrical language of F-theory such 7-branes are characterized by complex codimension one singularities in the structure of the elliptic fibration. Such codimension one singularities were systematically analyzed by Kodaira [8] well before the advent of F-theory. For a base of complex dimension one, such singularities are characterized by the familiar ADE classification of simple Lie algebras. For each type of codimension one singularity, the low-energy gauge group contains a local factor with the associated nonabelian Lie algebra. When the base is of higher dimension, monodromies around these codimension one loci can give rise to non-simply laced groups as well as the simply-laced groups found on bases of dimension one [9].

While the geometry of gauge groups is well understood in F-theory, the geometry of matter representations in such theories has only been worked out in a limited set of cases, and there is no general classification of the range of possibilities. Many types of matter representations can arise from local codimension two singularities in the elliptic fibration in the F-theory picture. Other types of matter (such as matter in the adjoint representation of  $SU(N)$ ) can arise from the global structure of the divisor locus [10, 11]. For the simplest types of representations, such as the fundamental representation of ADE groups, or the two-index antisymmetric representation of  $SU(N)$ , matter fields arise from a local rank one enhancement of the singularity structure, and the matter content is easily determined from a decomposition of the adjoint representation of the correspondingly enhanced group, as described by Katz and Vafa [12]. When the singularity structure of the elliptic fibration becomes more intricate, the associated matter representations become more exotic. Other examples associated with rank one enhancement were worked out in [9, 12, 13, 14]. In this paper we consider rank one enhancements as well as other kinds of singularity structures. In some cases the apparent Kodaira singularity associated with a coordinate transverse to the brane does not need to be completely resolved for the elliptic fibration to become smooth. In other cases, the local enhancement of the gauge group increases the rank by more than one. By carefully analyzing the local structure of such singularities, we can see how the resolution of the geometry gives rise to matter in a natural generalization of the rank one enhancement mechanism. When the codimension one locus in the base carrying a local

factor of the gauge group itself becomes singular, corresponding to a singular geometry for the 7-branes themselves, matter representations are possible that cannot be realized through elliptic fibrations whose nonabelian gauge symmetry corresponds to a smooth component of the discriminant locus.

The specific local singularity types we consider in this paper are motivated by global constructions. We develop a general analysis of F-theory Weierstrass models for theories with  $SU(N)$  gauge group localized on a generic divisor  $\sigma$  on a generic base  $B$ . As  $N$  increases, the set of possible singularity structures for the Weierstrass model becomes more complicated. While we do not complete the general analysis of all possibilities, we systematically show how different singularity types can arise through different choices of algebraic structure for the Weierstrass model. (This analysis complements the results of [15], where the form of the Weierstrass model is determined for large  $N$ .) We then apply this general analysis to the specific cases of 6D and 4D F-theory models on bases  $\mathbb{P}^2$  and  $\mathbb{P}^3$ .

In six dimensions, the space of allowed supergravity theories is strongly constrained by anomalies and other simple features of the low-energy theory [13, 14, 16, 17, 18, 19, 20, 21]. We can therefore combine the classification of theories from low-energy constraints with the analysis of singularity structures in global F-theory models to develop a fairly complete picture of the set of allowed matter representations in 6D quantum supergravity theories and their realizations through F-theory. In particular, when  $\sigma$  is a degree one curve (complex line) on  $\mathbb{P}^2$  we are able to reproduce all possible matter configurations for an  $SU(N)$  gauge group compatible with anomaly conditions.

The structure of the space of 4D F-theory constructions and possible matter representations for an  $SU(N)$  theory is closely parallel to the 6D story; though fewer constraints are understood from low-energy considerations in four dimensions, similar restrictions appear on matter representations arising in F-theory constructions. The work presented here represents some first steps towards a systematic understanding of the structure of matter in the global space of supergravity theories arising from F-theory compactifications.

In Section 2 we give the results of a local analysis for a variety of codimension two singularities associated with matter transforming under an  $SU(N)$  gauge group. We summarize the geometric resolution and group theory in each case, with details of the calculations given in an Appendix. In Section 3 we develop the general structure of Weierstrass models with gauge group  $SU(N)$  realized on a specific divisor. We use this general analysis in Section 4 to explicitly construct classes of global models in 6D without tensor multiplets associated with F-theory compactifications on  $\mathbb{P}^2$ , and in Section 5 to construct some 4D models associated with F-theory on  $\mathbb{P}^3$ . Section 6 contains concluding remarks and discussion of further directions and related open questions.

As this work was being completed we learned of related work on codimension two singularities by Esole and Yau [22].

## 2. Local analysis of codimension two singularities

The matter structure associated with any elliptic fibration can be understood through a

local analysis of the singularity structure of the fibration. Such a local analysis involves the simultaneous resolution of all singularities in the elliptic fibration along the lines of [23]. The way in which matter arises in F-theory can be understood from the related geometry of matter in type IIA compactifications [10] and in M-theory compactifications as discussed by Witten [11]. Generally, matter fields arise from  $\mathbb{P}^1$ 's in a smooth Calabi-Yau that have been shrunk to vanishing size in the F-theory limit. When these  $\mathbb{P}^1$ 's arise over codimension two loci in the F-theory base they correspond to local codimension two singularities giving rise to localized matter. In addition to the matter arising from local singularities, there are also global contributions to the matter content from  $\mathbb{P}^1$ 's that live in continuous families over the divisor  $\sigma$  in the base supporting the local factor of the gauge group. For example, in a 6D model there are  $g$  adjoint matter fields for  $SU(N)$ , where  $g$  is the genus of the curve defined by  $\sigma$ . We focus in this paper on the local contributions to the matter content, though as we discuss in Section 2.3, global matter contributions can become local, for example when  $\sigma$  develops a node. In this section we describe the detailed local geometry of matter in some representations of the gauge group  $SU(N)$ , which is associated with a local  $A_{N-1}$  singularity on a codimension one locus (divisor)  $\sigma$  in the F-theory base  $B$ .

We will describe several different classes of singularities in the discussion in this section. We begin with the simplest types of singularities, where the matter content can be understood through the standard Katz–Vafa [12] analysis, and then consider cases where the codimension two enhanced singularity is incompletely resolved. We then discuss cases where the relevant component of the discriminant locus itself is singular.

In this paper we use explicit geometric methods to analyze F-theory singularities. Recently Donagi and Wijnholt [24] and Beasley, Heckman, and Vafa [25] have developed an approach to resolving singularities on intersecting 7-branes based on normal bundles and a topological field theory on the world-volume of the intersection. It would be interesting to develop a better understanding of how the analyses of this paper can be understood from the point of view of the topological field theory framework.

To fix notation, we will be describing a local elliptic fibration characterized by a Weierstrass model

$$y^2 = x^3 + fx + g \tag{2.1}$$

where  $f, g$  are local functions on a complex base  $B$ . We choose local coordinates  $t, s$  on the base  $B$  so that the gauge group  $SU(N)$  arises from a codimension one  $A_{N-1}$  singularity on the locus  $\sigma(t, s) = 0$ . For compactification on an elliptically fibered Calabi-Yau threefold,  $s, t$  are the only two local coordinates needed on the base. For 4D theories associated with a Calabi-Yau fourfold, another coordinate  $u$  is needed for the base. This additional coordinate plays no rôle in the analysis in this section. In the simplest (smooth locus  $\{\sigma = 0\}$ ) cases, we can choose local coordinates with  $\sigma = t$ , so that the codimension one singularity arises at  $t = 0$  and the codimension two singularity of interest arises at the coordinate  $s = 0$ . In general, the Weierstrass form (2.1) of an  $A_{N-1}$  singularity describes a singularity associated with a double root at  $x = x_0$  in the elliptic fiber, where  $3x_0^2 + f(t = 0) = 0$ , so that it is convenient to change coordinates to  $x' = x - x_0$ . The singularity then arises at  $x' = 0$ ,

though the description of the elliptic fibration then contains an  $x^2$  term on the RHS of (2.1). This ‘‘Tate form’’ of the description of the elliptic fibration is often used in the mathematical analysis of singular elliptic fibrations [26, 9, 15], but is less convenient for a global description of the elliptic fibration in the context of F-theory, where the Weierstrass form allows a systematic understanding of the degrees of freedom associated with moduli of the physical theory. Some analyses of matter content associated with codimension two singularities related to constructions we consider here are also considered in [27] from the spectral cover point of view.

## 2.1 Standard rank one enhancement: $A_3 \rightarrow D_4$

In the simplest cases, matter arises from a codimension two singularity in which the  $A_{N-1}$  singularity, which is associated with a rank  $N-1$  gauge group, is enhanced to a singularity such as  $A_N$  or  $D_N$  of one higher rank. Such matter is characterized by the breaking of the adjoint of the corresponding rank  $N$  group\* through an embedding of  $A_{N-1}$ , as described in [9, 12]. In particular, matter in the fundamental ( $\square$ ) representation can be realized through a local codimension two singularity enhancement  $A_{N-1} \rightarrow A_N$  and matter in the two-index antisymmetric ( $\square$ ) representation (for which we will sometimes use the shorthand notation  $\Lambda^2$ ) can be realized through the enhancement  $A_{N-1} \rightarrow D_N$ . Matter in the three-index antisymmetric ( $\square$  or  $\Lambda^3$ ) representation can also be realized for  $SU(6)$ ,  $SU(7)$ , and  $SU(8)$  through local enhancement  $A_5 \rightarrow E_6$  [9, 12, 14],  $A_6 \rightarrow E_7$  [12, 14] and  $A_7 \rightarrow E_8$  [14].

As a simple example of this kind of singularity enhancement consider a Weierstrass model for the codimension two singularity enhancement  $A_3 \rightarrow D_4$ . Though the basic physics of the matter associated with this configuration are well understood, we go through the details as a warmup for more complicated examples. We consider an  $A_3$  singularity on the locus  $\sigma = t = 0$  with a  $D_4$  singularity at  $s = 0$ , given by the Weierstrass form (2.1) with

$$\begin{aligned} f &= -\frac{1}{3}s^4 - t^2 \\ g &= \frac{2}{27}s^6 + \frac{1}{3}s^2t^2. \end{aligned} \tag{2.2}$$

This particular form for  $f, g$  is chosen to match a form of this singularity that appears in the general global Weierstrass analysis in the next section of the paper. The  $A_3$  form of the singularity follows from the standard Kodaira classification [8, 3], since at generic  $s \neq 0$   $f, g$  have degree 0 in  $t$ , while the discriminant

$$\Delta = 4f^3 + 27g^2 = -s^4t^4 - 4t^6 \tag{2.3}$$

is of degree 4. At  $s = 0$ ,  $f$  has degree 2 and the discriminant has degree 6, so we have a  $D_4$  singularity.

---

\*We stress that this is not in general an enhancement of the gauge symmetry group. However, the adjoint breaking provides a convenient dictionary for the combinatorics involved, which works because in special cases there *is* a related gauge symmetry enhancement and Higgs mechanism.

As mentioned above, it is convenient to change coordinates

$$x \rightarrow x + \frac{1}{3}s^2 \quad (2.4)$$

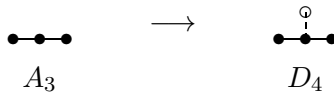
to move the singularity to  $x = 0$ . The Weierstrass equation then becomes

$$\Phi = -y^2 + x^3 + s^2x^2 - t^2x = 0. \quad (2.5)$$

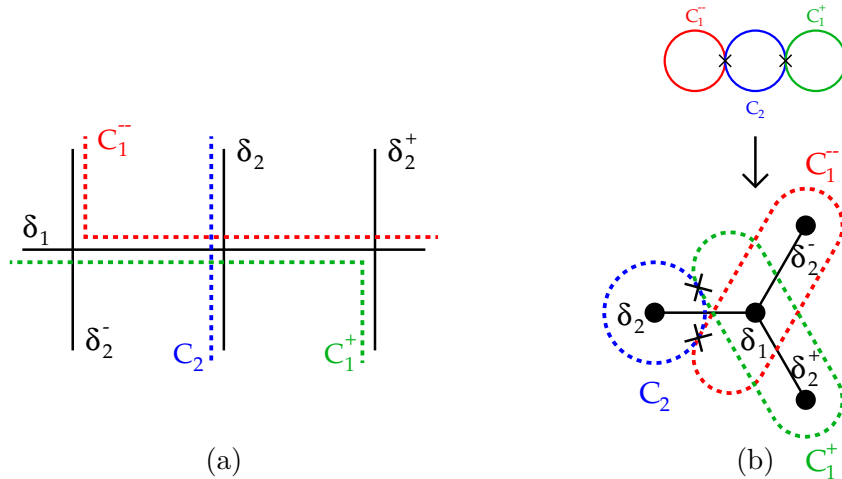
This gives a local equation for the Calabi-Yau threefold described by an elliptic fibration in coordinates  $(x, y, t, s) \in \mathbb{C}^2 \times \mathbb{C}^2$  where  $x, y$  are (inhomogeneous) local coordinates on the elliptic fiber living in  $\mathbb{P}^{2,3,1}$  and  $s, t$  are local coordinates on the base  $B$ .

An explicit analysis of the singularity resolution of the Calabi-Yau threefold defined by (2.5) is given in Section A.1 of the Appendix. Even in this rather simple case, the details of the resolution are slightly intricate. At a generic point  $s \neq 0$  along the  $A_3$  singularity  $\sigma$ , a blow-up in the transverse space gives two  $\mathbb{P}^1$ 's ( $C_{\pm}$ ) fibered over  $\sigma$ , which intersect at a singular point for each  $s$ . A further blow-up gives a third  $\mathbb{P}^1$  ( $C_2$ ) fibered over  $\sigma$ , which intersects each of  $C_{\pm}$ , giving a realization of the Dynkin diagram  $A_3$  in terms of the intersections of these curves. At  $s = 0$ , the resolution looks rather different. The first blow-up gives a single curve  $\delta_1$ , which both  $C_+, C_-$  approach in the limit  $s \rightarrow 0$ . A further blow-up at a singular point on  $\delta_1$  gives  $\delta_2 \sim C_2$ , and codimension two conifold-type double point singularities occur at two other points on  $\delta_1$ . Each of these codimension two singularities has two possible resolutions, giving four possible smooth Calabi-Yau threefold structures related by flops. In each resolution an additional  $\mathbb{P}^1$  is added at  $s = 0$ , completing the  $D_4$  Dynkin diagram. An example of how the curves  $C_a$  at generic  $s$  converge to the curves  $\delta_b$  at  $s = 0$  for one of the four combinations of resolutions is shown graphically in Figure 1.

The additional matter associated with the  $D_4$  can be understood by embedding  $A_3 \subset D_4$  and decomposing the adjoint of  $D_4$  into irreducible representations of  $A_3$ . The roots in the adjoint of  $D_4$  correspond to distinct  $\mathbb{P}^1$ 's at  $s = 0$  in the resolved Calabi-Yau. The subset of these roots corresponding to the adjoint of  $A_3$  are associated with the  $SU(4)$  vector bosons, and the remainder are matter fields. The adjoint of  $D_4$  decomposes into irreducible representations of  $A_3$  as  $\mathbf{28} \rightarrow \mathbf{15} + \mathbf{6} + \bar{\mathbf{6}} + \mathbf{1}$ . In a 6D theory, matter hypermultiplets live in quaternionic representations of the gauge group. The  $\mathbf{6}$  and  $\bar{\mathbf{6}}$  combine into a single quaternionic matter hypermultiplet in the  $\Lambda^2$  representation of  $A_3$  in 6D. An easy way to see that this representation appears is from the Dynkin diagram description of the embedding  $A_3 \subset D_4$ . (The embedding shown in Figure 1 is equivalent to this embedding under an isomorphism of  $D_4$ .)



The Dynkin weight  $[0, 1, 0]$  is the highest weight of the  $\Lambda^2$  representation of  $A_3$ . The  $\mathbb{P}^1$  associated with this state is precisely the extra (empty) node added to form  $D_4$  from  $A_3$  in



**Figure 1:** Embedding of  $A_3 \rightarrow D_4$  singularity encoded in eq. (A.23). Curves in  $D_4$  are depicted in black solid lines, while  $A_3$  curves are in colored dashed lines. Two different methods are used to depict the same embedding. (a) depicts each curve as a line, with intersections associated with crossings, as in much mathematical literature. (b) depicts  $D_4$  curves in Dynkin diagram notation, with nodes for curves and lines for intersection, and depicts  $A_3$  curves as colored dashed curves depicting  $\mathbb{P}^1$ 's at generic  $s$  and limit as  $s \rightarrow 0$ , with intersections denoted by “x”'s. There are four possible embeddings depending upon choices for codimension two resolutions. Choice depicted has  $\tau_+ = 1, \tau_- = 0$ , according to notation in Section A.1 of Appendix, so for example  $C_1^+ \rightarrow \delta_1 + \delta_2^+$  as  $s \rightarrow 0$ .

this embedding. The weight of this state can be determined from the intersection numbers of this  $\mathbb{P}^1$  with the roots of  $A_3$ ; the additional  $\mathbb{P}^1$  has intersection number 1 with the middle root of  $A_3$  and no intersection with the other roots. (See [28] for a review of the notation of Dynkin weights and the relevant group theory.)

## 2.2 Incomplete and complete resolutions

We now consider a slightly more complicated set of enhancements of an  $A_{N-1}$  codimension one singularity. In this case we consider the enhancement of  $A_5$  by various types of local singularities and the associated matter content. We will begin with the example of  $A_5$  enhanced to  $D_6$  through a standard rank one enhancement quite similar to the preceding analysis of  $A_3 \rightarrow D_4$ . This again gives a matter field in the  $\Lambda^2$  antisymmetric representation. We will then consider the effect of a local  $E_6$  singularity. Depending upon the degree of vanishing of certain terms in the local defining equation, the  $E_6$  can either be incompletely resolved or can be completely resolved in the threefold. The  $E_6$  singularity gives rise to matter in the three-index antisymmetric ( $\Lambda^3$ ) representation; in the 6D context we get a half or full hypermultiplet in this representation depending on whether the singularity is completely resolved.

In each case, we choose a non-generic Weierstrass model, with a specific form motivated by the global analysis carried out in the following section.



### 2.2.1 Enhancement $A_5 \subset D_6$

We begin with the Weierstrass coefficients

$$\begin{aligned} f &= -\frac{1}{3}s^4 - 2s^3t + (2s^2 - 3)t^2 + 3t^3, \\ g &= \frac{2}{27}s^6 + \frac{2}{3}s^4t + (2s^2 - \frac{2}{3}s^4)t^2 + (2 - 3s^2)t^3 + (s^2 - 3)t^4. \end{aligned} \quad (2.6)$$

These describe an  $A_5$  singularity on the locus  $t = 0$  enhanced to a  $D_6$  singularity at  $s = 0$ , where the orders of vanishing of  $f, g, \Delta$  are 2, 3, 6. Changing variables through

$$x \rightarrow x + \frac{1}{3}s^2 + t \quad (2.7)$$

gives the local equation

$$\Phi = -y^2 + x^3 + s^2x^2 + 3x^2t + 3t^3x + 2s^2t^2x + s^2t^4 = 0. \quad (2.8)$$

An analysis much like that of  $A_3 \subset D_4$ , summarized in Section A.2.1 of the Appendix, shows that this singularity is resolved to give a set of curves with  $D_6$  structure at  $s = 0$ , giving matter in the  $\Lambda^2$  representation of  $A_5$  with highest weight vector having Dynkin indices  $[0, 1, 0, 0, 0]$ .

### 2.2.2 Enhancement $A_5 \subset E_6$

We now consider a situation where  $A_5$  is enhanced to  $E_6$ . The local model we consider is closely related to (2.8). We begin with the Weierstrass coefficients

$$\begin{aligned} f &= -\frac{1}{3}\rho^4 - 2\rho^3t + (2\rho - 3\rho^2)t^2 + 3t^3, \\ g &= \frac{2}{27}\rho^6 + \frac{2}{3}\rho^5t + (2\rho^4 - \frac{2}{3}\rho^3)t^2 + (2\rho^3 - 3\rho^2)t^3 + (1 - 3\rho)t^4. \end{aligned} \quad (2.9)$$

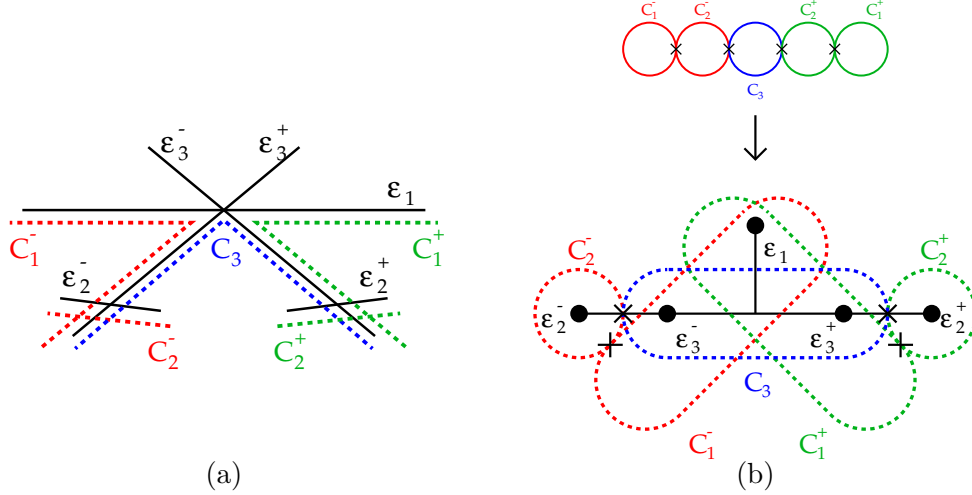
Changing variables through

$$x \rightarrow x + \frac{1}{3}\rho^2 + \rho t \quad (2.10)$$

gives

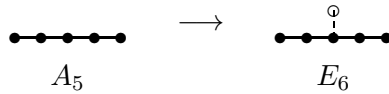
$$\Phi = -y^2 + x^3 + \rho^2x^2 + 3\rho x^2t + 3t^3x + 2\rho t^2x + t^4 = 0. \quad (2.11)$$

We describe explicit global 6D models in which this singularity structure arises in Section 4. In (2.11), the parameter  $\rho$  can be either  $\rho = s$  or  $\rho = s^2$ . The detailed analysis of the singularity resolution in both cases is carried out in Section A.2.2 of the Appendix. To understand the results of this analysis it is helpful to clarify the structure of the  $E_6$  singularity at  $s = 0$ . The Kodaira classification of singularities is really only applicable in the context of codimension one singularities. For generic  $s$ , we can take a slice at constant  $s$ , giving a codimension one singularity of type  $A_5$  on each slice intersecting the curve at  $t = 0$ . To determine the type of singularity at  $s = t = x = y = 0$ , we are considering a slice at  $s = 0$ . Just because there is a singularity in this slice, however, does not mean that the full Calabi-Yau threefold is singular. In particular, in the case at hand, when  $\rho = s$ ,



**Figure 2:** Embedding  $A_5 \rightarrow E_6$  with incomplete resolution of  $E_6$  singularity in threefold.

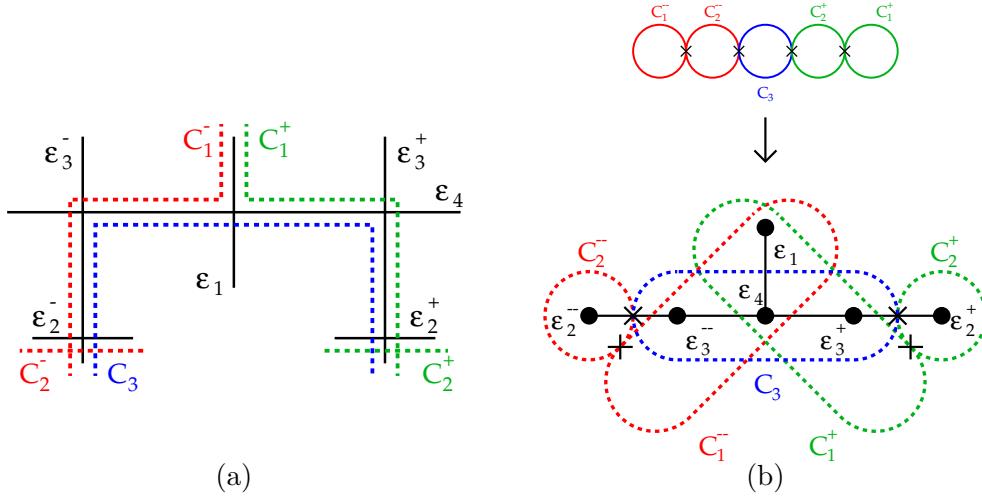
systematically blowing up the singularity at the origin allows the Calabi-Yau threefold to be smoothed before the full  $E_6$  singularity has been resolved. At the final stage of this resolution process, there is an apparent singularity in the slice at  $s = 0$  but the full threefold has no singularity. A diagram depicting the blown-up  $\mathbb{P}^1$ 's away from  $s = 0$  ( $C_a$ 's) and at  $s = 0$  ( $\epsilon_b$ 's) for the incomplete  $E_6$  resolution from  $\rho = s$  is shown in Figure 2. When  $\rho = s^2$ , the full  $E_6$  singularity is resolved, giving the configuration depicted in Figure 3. Although this explicit singularity resolution gives an embedding of  $A_5 \subset E_6$  with a somewhat unconventional appearance, this embedding is unique up to automorphisms of  $E_6$ , so is equivalent to the embedding associated with extending the Dynkin diagram  $A_5$  by adding a new node attached to middle node of the  $A_5$  to form the  $E_6$  diagram.



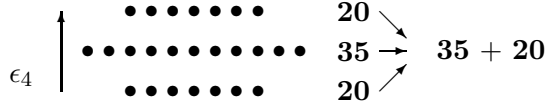
Let us now consider the matter content in each of these situations. In the fully resolved  $E_6$ , we have the usual story of rank one enhancement and the adjoint of  $E_6$  decomposes under  $A_5 \subset E_6$  as

$$\mathbf{78} = 3 \cdot \mathbf{1} + \mathbf{35} + 2 \cdot \mathbf{20}. \quad (2.12)$$

This gives matter in the 3-index antisymmetric ( $\Lambda^3$ )  $\mathbf{20}$  representation of  $A_5$ . Again, the appearance of this matter representation is apparent from the Dynkin index  $[0, 0, 1, 0, 0]$  associated with the intersection of the added node with the original nodes of the  $A_5$ . The possibility of this kind of matter associated with a local  $E_6$  enhancement was previously discussed in [9, 12, 14]. In a 6D theory, as in the  $\Lambda^2$  matter story, the two  $\mathbf{20}$ 's combine into a single full hypermultiplet. Because the  $\mathbf{20}$  is by itself already a quaternionic representation of  $A_5$ , however, this can also be thought of as two half-hypermultiplets.



**Figure 3:** Embedding  $A_5 \rightarrow E_6$  with complete resolution of  $E_6$  singularity in threefold.



**Figure 4:** A schematic depiction of the decomposition of the adjoint of  $E_6$  under the action of  $A_5$ . The action of  $A_5$  is taken to be in the horizontal direction. The root  $\epsilon_4$  is perpendicular to all roots of  $A_5$ . In the incompletely resolved  $E_6$ , a projection is taken in the  $\epsilon_4$  direction that combines the two  $\mathbf{20}$ 's of  $A_5$  into a single half hypermultiplet.

Now we consider the case where the  $E_6$  is incompletely resolved. In this case, the set of roots of  $E_6$  are not all associated with  $\mathbb{P}^1$ 's in the full Calabi-Yau over the point  $s = 0$ . Thus, the amount of matter is reduced. The root of  $E_6$  that is not blown up, associated with the curve  $\epsilon_4$  in the complete resolution depicted in Figure 3, is orthogonal to all roots of  $A_5$ . For example,  $\epsilon_4 \cdot C_1^+ = \epsilon_4 \cdot (\epsilon_1 + \epsilon_3^+ + \epsilon_4) = -2 + 1 + 1 = 0$ . We can therefore describe the matter content of the incompletely resolved  $E_6$  by projecting in the direction parallel to  $\epsilon_4$ . This collapses the two  $\mathbf{20}$ 's into a single matter representation (see Figure 4). In the 6D theory this gives a half-hypermultiplet in the  $\Lambda^3$  representation. It was also noted in [12] that the appearance of a quadratic parameter like  $\rho = s^2$  in the defining equation of the singularity is associated with a pair of half-hypermultiplets in certain situations; this observation matches well with the appearance of a single half-hypermultiplet when  $s^2$  is replaced with  $s$ .

It is interesting to understand how the intersection properties of the  $C$  curves from  $A_5$  are realized in the incomplete  $E_6$  resolution. The detailed expansion of the  $C$ 's in terms of the roots  $\epsilon$  of the  $E_6$  is given in (A.53), and shown graphically in Figure 2. In the incompletely resolved  $E_6$ , we can consider the geometry of the slice at  $s = 0$  containing

blown-up  $\mathbb{P}^1$ 's associated with all roots of  $E_6$  other than  $\epsilon_4$ . In this slice, there is a  $\mathbb{Z}_2$  singularity at the intersection point of  $\epsilon_1, \epsilon_3^\pm$ . This point contributes only  $1/2$  to the Euler characteristic of spaces in which it is contained. Each of the curves intersecting the point consequently has a self-intersection given by  $\epsilon_1 \cdot \epsilon_1 = -3/2$ , *etc.* and the intersection between each pair of curves meeting at this point is  $1/2$ , so  $\epsilon_1 \cdot \epsilon_3^\pm = 1/2$ , *etc.*. We see that the linear combinations of these singular curves spanned by the  $C$ 's preserve the correct intersection rules for  $A_5$ ; for example,

$$C_1^+ \cdot C_3 = (\epsilon_1 + \epsilon_3^+) \cdot (\epsilon_3^+ + \epsilon_3^-) = -3/2 + 3(1/2) = 0, \quad (2.13)$$

$$C_3 \cdot C_3 = (\epsilon_3^+ + \epsilon_3^-) \cdot (\epsilon_3^+ + \epsilon_3^-) = 2(-3/2) + 2(1/2) = -2. \quad (2.14)$$

We expect that there are many types of codimension two singularities that can appear in F-theory with analogous descriptions in terms of incomplete resolutions. In Section 4 we describe global 6D F-theory models in which this kind of incomplete resolution appears explicitly, affecting the matter content of the theory.

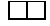
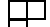

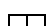
## 2.3 Matter on a singular 7-brane

For the fundamental and multi-index antisymmetric representations of  $SU(N)$  that we have studied so far, the associated F-theory geometry involves the enhancement at a codimension two locus of an  $A_{N-1}$  singularity living on a 7-brane that itself is wrapped on a smooth codimension one locus in the base. Other kinds of representations can arise when the 7-branes are wrapped on a singular divisor. In [29], Sadov gave some evidence suggesting that a two-index symmetric ( $\square$  or  $\text{Sym}^2$ ) representation of  $SU(N)$  should arise when the gauge group is realized on a codimension one space having an ordinary double point singularity. The connection between matter representations and geometric singularities can be made much more general from analysis of anomaly cancellation in 6D theories. We describe the general connection that we expect between matter representations and singularities in the 7-brane configuration, and then describe in some detail the case of the ordinary double point singularity from this point of view.

### 2.3.1 Representation theory and singularities

It was found in [20] that associated with each representation of  $SU(N)$  there is a numerical factor  $g_R$  that corresponds in a 6D F-theory model to a contribution to the genus of the divisor associated with the  $SU(N)$  local factor. The analysis in [20] was based on compactifications on  $\mathbb{P}^2$ , but the result can be stated more generally. From the anomaly cancellation conditions for an F-theory construction on an arbitrary base (see [5] for a review), the genus  $g$  of the curve  $C$  on which the 7-branes associated with any  $SU(N)$  local factor of the gauge group are wrapped can be written in terms of a sum over contributions from each matter representation

$$2g - 2 = (K + C) \cdot C = \sum_R x_R g_R - 2, \quad (2.15)$$

Rep.	Dimension	$A_R$	$B_R$	$C_R$	$g_R$
Adjoint	$N^2 - 1$	$2N$	$2N$	6	1
	$\frac{N(N+1)}{2}$	$N + 2$	$N + 8$	3	1
	$\frac{N(N^2-1)}{3}$	$N^2 - 3$	$N^2 - 27$	$6N$	$N - 2$
	$\frac{N(N+1)(N+2)}{6}$	$\frac{N^2+5N+6}{2}$	$\frac{N^2+17N+54}{2}$	$3N + 12$	$N + 4$
	$\frac{N^2(N+1)(N-1)}{12}$	$\frac{N(N-2)(N+2)}{3}$	$\frac{N(N^2-58)}{3}$	$3(N^2 + 2)$	$\frac{(N-1)(N-2)}{2}$

**Table 1:** Values of the group-theoretic coefficients  $A_R, B_R, C_R$ , dimension and genus for some representations of  $SU(N)$ ,  $N \geq 4$ .

where  $x_R$  is the number of matter hypermultiplets in representation  $R$ , and the genus contribution of a given representation is defined to be

$$g_R = \frac{1}{12} (2C_R + B_R - A_R) . \quad (2.16)$$

In this formula,  $A_R, B_R, C_R$  are group theory coefficients defined through

$$\text{tr}_R F^2 = A_R \text{tr} F^2 \quad (2.17)$$

$$\text{tr}_R F^4 = B_R \text{tr} F^4 + C_R (\text{tr} F^2)^2 , \quad (2.18)$$

where  $\text{tr}_R$  denotes the trace in representation  $R$ , while  $\text{tr}$  without a subscript denotes the trace in the fundamental representation. A table of group theory coefficients and genera for some simple  $SU(N)$  representations appears in [20]; we reproduce here the part of the table describing representations with nonzero genus in Table 1. All single-column antisymmetric representations ( $\Lambda^2, \Lambda^3, \dots$ ) have vanishing genus.

While we have described so far the relationship between representation theory and geometry of singularities only for  $SU(N)$  local factors and representations, a similar result holds for any simple local factor of the gauge group with the inclusion of appropriate numerical factors depending on the normalization of the trace. For a general gauge group the genus contribution is

$$g_R = \frac{1}{12} (2\lambda^2 C_R + \lambda B_R - \lambda A_R) , \quad (2.19)$$

where  $\lambda$  is a group-dependent normalization factor, with  $\lambda_{SU(N)} = 1, \lambda_{SO(N)} = 2$ , etc.; values of  $\lambda$  for all simple groups are listed in [19].

We now review some elementary features of plane curves (complex curves in  $\mathbb{P}^2$ ) that clarify the connection of the group theory structure just described with singularities in F-theory. For more background in the basic algebraic geometry of plane curves see, e.g., [30]. In algebraic geometry, a smooth plane curve is characterized by two invariants: the degree  $b$  of the polynomial defining the curve in  $\mathbb{P}^2$ , and the genus  $g$  of the curve, which is related to the Euler characteristic of the curve through the usual relation

$$\chi = 2 - 2g \quad (2.20)$$

For a smooth plane curve, the degree and genus are related by

$$2g = (b - 1)(b - 2). \quad (2.21)$$

Thus, lines ( $b = 1$ ) and conics ( $b = 2$ ) have genus 0, smooth cubics ( $b = 3$ ) are elliptic curves of genus 1, curves of degree 4 have genus 3, etc.

Using inhomogeneous coordinates  $t, s$  on  $\mathbb{P}^2$ , a curve  $f(t, s) = 0$  is singular at any point where

$$\partial f / \partial t = \partial f / \partial s = 0. \quad (2.22)$$

For example, the cubic

$$f(t, s) = t^3 + s^3 - st = 0 \quad (2.23)$$

is singular at the point  $(t, s) = (0, 0)$ , and locally takes the form  $st = 0$ , describing two lines crossing at a point.

For a singular curve, there are two distinct notions of genus that become relevant. The *arithmetic* genus is given by (2.21) for any curve, singular or nonsingular. The *geometric* genus (which we denote by  $p_g$ ) is the topological genus of a curve after all singularities have been appropriately smoothed. For example, the singularity in (2.23) is known as an *ordinary double point* singularity, where two smooth branches of the curve cross at a point. This singularity can be removed by blowing up the origin to a  $\mathbb{P}^1$ , which separates the two points, giving a curve of geometric genus 0. In general, the arithmetic and geometric genera of a plane curve  $C$  with multiple singularities are related through

$$g = (b - 1)(b - 2)/2 = p_g + \sum_P \frac{m_P(m_P - 1)}{2}, \quad (2.24)$$

where the sum is over<sup>†</sup> all singular points  $P$  in  $C$ , and  $m_P$  is the multiplicity of the singularity at  $P$ . The multiplicity of an ordinary singularity where  $k$  branches of the curve cross at a common point is  $k$ . It is easy to see that deforming such a singularity leads to  $k(k - 1)/2$  ordinary double point singularities, each of which contributes one to the genus. More generally, the multiplicity of a singularity in a plane curve is given by the lowest power of a monomial appearing in the polynomial defining the curve in local coordinates around the singularity. For example, for degree 3 curves, in addition to the ordinary double point type of singularity encountered in (2.23), a *cuspidal* (non-ordinary) double point singularity can arise at points like the origin in the cubic

$$f(t, s) = t^3 - s^2 = 0. \quad (2.25)$$

The multiplicity of such a cusp singularity is 2; this cusp can be found as a degenerate limit of the class of cubics with ordinary double point singularities  $t^3 + at^2 - s^2 = 0$  as  $a \rightarrow 0$ . Note that a curve of geometric genus 0 is a *rational* curve, meaning that the curve can be parameterized using rational functions. For example, (2.25) has arithmetic genus 1 but

---

<sup>†</sup>There is an important subtlety here: after blowing up a singular point, there may still be singular points in the inverse image of the original point, and they must be blown up as well, *ad infinitum*. The sum in (2.24) must include these “infinitely near” points.

geometric genus 0, and can be parameterized as  $t = a^2, s = a^3$ . For higher degree curves, more exotic types of singularities can arise with higher intrinsic multiplicities. While an ordinary double point singularity is resolved by a single blow-up, as the singularity becomes more extreme, the point must be blown up more times to completely resolve the singularity. From (2.24), we see that the total arithmetic genus of a curve has a contribution from the geometric genus and also a contribution from the various singular points in the curve.

We now return to the discussion of matter and singularities in the F-theory context. The genus appearing in (2.15) is the arithmetic genus. For a local factor of the gauge group associated with 7-branes on a smooth curve, there are  $g$  matter fields in the adjoint representation, associated with  $\mathbb{P}^1$ 's in the resolved space that are free to move over the curve of genus  $g$ . Since the adjoint representation has  $g_R = 1$ , these non-localized adjoint matter fields saturate (2.24); a gauge group realized on a smooth curve can thus only have local matter in the fundamental and multi-index antisymmetric representations. If the gauge group lives on a singular curve, however, the number of adjoint representations is given by  $p_g$ , with the type of singularities in the curve determining the types of additional matter that can arise. From (2.24), we expect that a matter representation  $R$  will be associated with a localized singularity in  $\sigma$  contributing  $g_R$  to the genus. This gives a clear picture of how matter representations should be associated with singular divisor classes in F-theory.

For example, consider the symmetric ( $\text{Sym}^2$ ) representation of  $SU(N)$ . This representation has  $g_{\text{Sym}^2} = 1$  and should be associated with a singularity of multiplicity 1. This matches with Sadov's prediction that such matter should be associated with an ordinary double point in  $\sigma$ . We analyze this type of singularity in detail in the following section. As another example, consider the ‘‘box’’ ( $\boxplus$ ) representation of  $SU(4)$ . From Table 1, we see that this representation has genus  $g_R = 3$ . Thus, we expect that it will be produced by a singularity of multiplicity 3 in the divisor locus carrying a stack of 7-branes in a 6D F-theory model on  $\mathbb{P}^2$ . In [20] it was shown that this representation can arise in apparently consistent 6D supergravity models with  $SU(4)$  gauge group and no tensor multiplets. We discuss this representation further in Section 2.4.2.

Although the preceding discussion was based on the analysis of 6D supergravity models, where anomaly cancellation strongly constrains the range of possible models, the connection between the group theoretic genus contribution of a given matter representation and the corresponding singularity type in the F-theory picture should be independent of dimension. Thus, in particular, the same correspondence will relate matter in 4D supergravity models to localized codimension two singularity structures in F-theory compactifications on a Calabi-Yau threefold, just as the Kodaira classification describes gauge groups based on codimension one singularities in all dimensions.

### 2.3.2 Ordinary double point singularities

We now consider the simplest situation where the locus  $\sigma$  on which the 7-branes are wrapped itself becomes singular in a 6D F-theory model. This occurs when  $\sigma$  contains an ordinary double point singularity, such as arises at the origin for the curve  $u^3 + u^2 - v^2 = u^3 + (u + v)(u - v) = 0$ . Locally, an ordinary double point singularity takes the form

$st = 0$  in a local coordinate system; here this is the case with  $s = u + v, t = u - v$ . The geometry and physics of such an intersection is well-known. A stack of 7-branes associated with an  $A_{N-1}$  codimension one singularity that has a transverse intersection with a stack of 7-branes associated with an  $A_{M-1}$  singularity gives rise to matter in a bifundamental representation

$$(N, \bar{M}) + (\bar{N}, M) \text{ or } (N, M) + (\bar{N}, \bar{M}). \quad (2.26)$$

For two branes that intersect each other in only one place, and do not intersect other branes, these two representations are effectively indistinguishable, being equivalent under a redefinition of the gauge group on one of the branes. When the branes have multiple intersections, or are identified, however, the relative structure of representations from one intersection to another (or from one branch of the brane to another) means that these two distinct types of bifundamental representations must be distinguished. When the two stacks of 7-branes are actually the same, corresponding to a self-intersection of  $\sigma$ , the resulting representation of  $SU(N)$  is either an adjoint hypermultiplet, or a symmetric and an antisymmetric hypermultiplet ( $\Lambda^2 + \text{Sym}^2$ )

$$\begin{aligned} 1 + \text{adj} : & \quad \text{singlet}(1) + \text{adjoint}(N^2 - 1) \\ & \text{or} \\ \Lambda^2 + \text{Sym}^2 : & \quad \square(N(N - 1)/2) + \square\square(N(N + 1)/2). \end{aligned} \quad (2.27)$$

To understand which of these representations is realized, and to connect with the general discussion of matter and singularities, it is helpful to go through the F-theory singularity analysis in a similar fashion to that done for the singularities analyzed above. For concreteness, we describe the self-intersection of a curve  $\sigma$  carrying an  $A_3$  singularity in a 6D model.

To describe an  $SU(4)$  gauge group on a singular divisor class  $\sigma$ , we can substitute  $s \rightarrow 1, t \rightarrow \sigma$  in the equation (2.5) for an  $A_3$  singularity

$$\Phi = -y^2 + x^3 + x^2 - \sigma^2 x = 0. \quad (2.28)$$

For the local ordinary double point  $\sigma = st$ , we have

$$\Phi = -y^2 + x^3 + x^2 - s^2 t^2 x = 0. \quad (2.29)$$

This defines a Calabi-Yau threefold that is singular along the lines  $s = 0$  and  $t = 0$  with an enhancement to  $A_7$  at the point  $s = t = 0$ . We can resolve the singularity systematically by blowing up the curves along  $t = 0, s = 0$  and at the origin. The details are described in Section A.3. The result of this analysis is that the 3  $\mathbb{P}^1$ 's giving the  $A_3$  structure along each of the curves  $s = 0, t = 0$  are embedded into two orthogonal  $A_3$  subgroups of the  $A_7$  Dynkin diagram. The embedding found from explicit singularity resolution is equivalent to the canonical embedding of  $SU(4) \times SU(4) \subset SU(8)$  depicted in terms of Dynkin diagrams as

$$\begin{array}{ccc} \bullet\text{---}\bullet\text{---}\bullet & \times & \bullet\text{---}\bullet\text{---}\bullet \longrightarrow \bullet\text{---}\bullet\text{---}\circ\text{---}\bullet\text{---}\bullet\text{---}\bullet \\ A_3 \times A_3 & & A_7 \end{array}$$



We can then decompose the adjoint of  $A_7$  as usual to get the matter content. If the two  $SU(4)$  gauge groups were independent, this would give one of the bifundamental representations (2.26). When the two  $A_3$  singularity loci are connected, however, which of the matter representations (2.27) are realized depends upon the geometry of  $\sigma$ . Locally, the 3  $\mathbb{P}^1$ 's associated with simple roots of  $A_3$  on one branch can be labeled with 1, 2, 3. When this labeling is followed around  $\sigma$  onto the second branch, we have an embedding of a single  $A_3$  through

$$A_3 \rightarrow A_3 \times A_3 \rightarrow A_7 \quad (2.30)$$

that can be realized through either of the two possibilities

$$\begin{array}{ccc}
 \begin{array}{c} 1 \ 2 \ 3 \\ \bullet \bullet \bullet \\ A_3 \end{array} & \longrightarrow & \begin{array}{c} 1 \ 2 \ 3 \quad 1 \ 2 \ 3 \\ \bullet \bullet \bullet \circ \bullet \bullet \bullet \\ A_7 \end{array} \quad \text{or} \quad \begin{array}{c} 1 \ 2 \ 3 \quad 3 \ 2 \ 1 \\ \bullet \bullet \bullet \circ \bullet \bullet \bullet \\ A_7 \end{array}
 \end{array}$$

These two possibilities correspond to the two matter options (2.27).

Thus, we see that an ordinary double point singularity in  $\sigma$  can either be associated with an adjoint plus a singlet, or a symmetric and an antisymmetric matter multiplet. In each case, the contribution through (2.16) to the genus is 1, so either possibility is consistent with the general picture of the association between geometry and group theory.

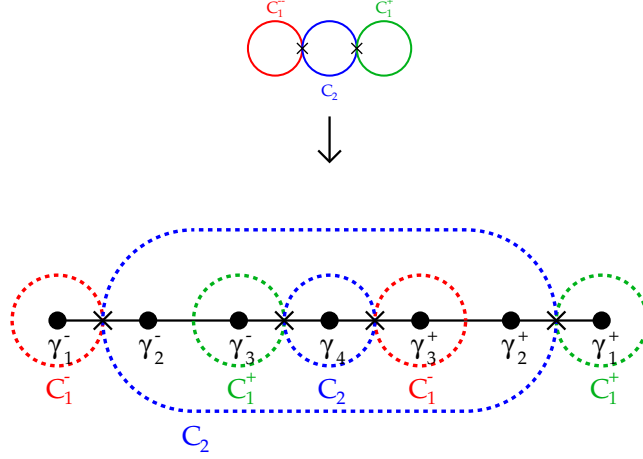
Which of the possible representations is realized, however, is determined by nonlocal features of the geometry. To see which of the embeddings from the diagram above is realized it is necessary to track the labeling of the  $A_3$  roots around a closed path in  $\sigma$  connecting the two branches that intersect. The information in the orientation of the ordering of these roots amounts to an additional  $\mathbb{Z}_2$  of information contained in the structure of any brane. It is interesting to note that this degree of freedom is present in any configuration of type II D-branes, although it is not generally discussed.

The explicit singularity resolution computed in Section A.3 is depicted graphically in Figure 5, for a particular choice of relative orientation of the  $A_3$  curves in the two branes. For this choice of orientation, the representation given is the symmetric + antisymmetric representation. This can be seen by computing the Dynkin weight of the curve  $\gamma_1^- + \gamma_2^- + \gamma_3^- + \gamma_4 + \gamma_3^+$ . The only nonzero inner product of this curve with  $C_1^\pm, C_2$  is

$$(\gamma_1^- + \gamma_2^- + \gamma_3^- + \gamma_4 + \gamma_3^+) \cdot C_1^- = -2. \quad (2.31)$$

The resulting Dynkin weight  $[-2, 0, 0]$  occurs in the (conjugate of the) symmetric representation, and not in the adjoint, so this embedding corresponds to the matter representation  $(\square + \square)$ .

One simple class of global models that contain ordinary double point singularities is the set of models where an  $A_N$  singularity is wrapped on a divisor class  $\sigma$  that has a self-intersection, but which can be continuously deformed into a smooth divisor class without changing the gauge group of the theory. In this case, the self-intersection is expected to generically be of the type that gives an adjoint representation, since there is no reason



**Figure 5:** Embedding of  $A_3 \rightarrow A_7$  at an ordinary double point singularity, giving a two-index symmetric representation as well as antisymmetric representation ( $\square + \square$ ).

to expect the type of matter to change discontinuously as the divisor becomes singular. We give an example of such a configuration in Section 4. In some cases, however, a more complicated global Weierstrass model can give self-intersections that produce symmetric and antisymmetric matter fields. The presentation of an explicit example of such a configuration is left for the future work.

## 2.4 Group theory of novel matter representations

The range of possible codimension two singularities in F-theory is very large, and provides an inviting territory for exploration. One guide in exploring this space is the set of matter representations that may be expected to arise from F-theory singularity structures based on analysis of low-energy theories. As we discuss in more detail in Section 4, a systematic analysis of  $SU(N)$  matter representations in 6D supergravity theories without tensor multiplets in [20] identified a number of representations that may arise in F-theory constructions. In this section we discuss the group theory aspect of how two of these representations may arise. Identification of local and global models for singularity structures realizing these matter representations is left for the future.

The two representations we focus on here are the 4-index antisymmetric ( $\Lambda^4$ ) representation of  $SU(8)$  with Young diagram  $\begin{array}{|c|} \hline \square \\ \hline \end{array}$  and the “box” representation of  $SU(4)$  with Young diagram  $\begin{array}{|c|c|} \hline \square & \square \\ \hline \end{array}$

### 2.4.1 4-index antisymmetric representation of $SU(8)$

To realize a representation  $R$  of a group  $G$  through the Katz–Vafa analysis,  $G$  must embed into a group  $G'$  of one rank higher, and the representation  $R$  must appear in the decomposition of the adjoint of  $G'$  under  $G \subset G'$ . At first appearance, this seems difficult for the  $\Lambda^4$  representation of  $SU(8)$ . There is a natural embedding of  $A_7$  into  $E_8$  associated with the obvious embedding of Dynkin diagrams

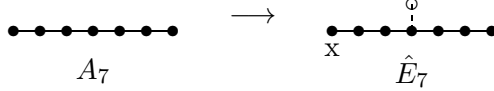


Under this embedding, the adjoint of  $E_8$  decomposes as [28]

$$248(\text{Adj}) \rightarrow 63(\text{Adj}) + \mathbf{1} + 28 \left( \begin{array}{|c|} \hline \square \\ \hline \end{array} \right) + \bar{28} + \left[ 8 \left( \square \right) + \bar{8} + 56 \left( \begin{array}{|c|} \hline \square \\ \hline \end{array} \right) + \bar{56} \right]. \quad (2.32)$$

The appearance of the  $\Lambda^3$  representation, corresponding to Dynkin indices  $[0, 0, 1, 0, 0, 0, 0]$  is clear from the geometry associated with the Dynkin diagram embedding depicted above. The  $\mathbb{P}^1$  associated with the extra (empty) circle in the  $E_8$  Dynkin diagram has inner product 1 with the  $\mathbb{P}^1$  associated with the third root in the  $A_7$  diagram, giving the Dynkin weight  $[0, 0, 1, 0, 0, 0, 0]$ .

In addition to the above embedding, however, there is a second, inequivalent embedding of  $A_7 \subset E_8$  [31, 32]. This alternate embedding can be understood through a sequence of maximal subgroup embeddings  $A_7 \subset E_7 \subset E_8$ . The form of the embedding  $A_7 \subset E_7$  can be understood through extended Dynkin diagrams. In general [33], a maximal subgroup  $H \subset G$  of simple Lie algebras is associated with an embedding of the Dynkin diagram of  $H$  into the *extended* Dynkin diagram of  $G$ . The embedding of  $A_7$  into the extended Dynkin diagram of  $E_7$  is depicted as (denoting the extra node extending the  $E_7$  with an “x”)



The diagram suggests that the decomposition of the  $E_7$  adjoint will include a state in an  $A_7$  representation with a Dynkin weight of  $[0, 0, 0, 1, 0, 0, 0]$ , which is the desired highest weight of the  $\Lambda^4$  representation. Indeed, under this embedding of  $A_7 \rightarrow E_7$  the adjoint decomposes as

$$133(\text{Adj}) \rightarrow 63(\text{Adj}) + 70 \left( \begin{array}{|c|} \hline \square \\ \hline \square \\ \hline \end{array} \right). \quad (2.33)$$

Using this embedding to further embed  $A_7 \subset E_7 \subset E_8$  gives the decomposition of the adjoint of  $E_8$

$$248(\text{Adj}) \rightarrow 63(\text{Adj}) + \mathbf{1} + 28 \left( \begin{array}{|c|} \hline \square \\ \hline \end{array} \right) + \bar{28} + \left[ \mathbf{1} + \bar{\mathbf{1}} + 28 + \bar{28} + 70 \left( \begin{array}{|c|} \hline \square \\ \hline \square \\ \hline \end{array} \right) \right]. \quad (2.34)$$

So under this embedding, the adjoint of  $E_8$  decomposes in a way that gives the  $\Lambda^4$  representation of  $A_7$ . Note that the representation content in brackets in (2.32), (2.34), giving the difference in content between the two decompositions, is given in the two cases by

$$\Lambda^1 + \Lambda^3 + \Lambda^5 + \Lambda^7 \quad \text{vs.} \quad \Lambda^0 + \Lambda^2 + \Lambda^4 + \Lambda^6 + \Lambda^8. \quad (2.35)$$

This is precisely the difference in representation content between the two spinor representations of  $SO(16)$  when decomposed under  $SU(8)$ .

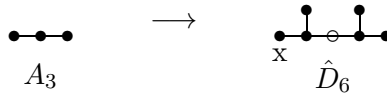
As we discuss further in Section 4, we anticipate that a further analysis of global 6D models with  $SU(8)$  gauge group will provide Weierstrass forms that locally contain singularities giving rise to matter in the  $\Lambda^4$  representation of  $SU(8)$ . The group theory structure just described is one natural way in which this may occur.

### 2.4.2 Box representation of $SU(4)$

Now let us consider the “box” representation of  $SU(4)$ . In terms of Dynkin indices, this representation is

$$\boxplus(\mathbf{20}') \leftrightarrow [0, 2, 0]. \quad (2.36)$$

This representation does not appear in the decomposition of the adjoint of any rank one gauge group enhancement. Since the genus (2.16) of the representation is nonzero, we expect this representation to arise from a Weierstrass singularity where the curve on the base supporting the singularity locus is itself singular. As in the ordinary double point giving matter in the adjoint and symmetric representations of  $SU(N)$  through the embedding  $A_{N-1} \rightarrow A_{N-1} \times A_{N-1} \rightarrow A_{2N-1}$ , we look for a similar multiple embedding that may give rise to the representation (2.36). As in the previous example, such an embedding can be realized through an embedding of  $A_3 \times A_3$  into the extended Dynkin diagram for  $D_6$



Under this embedding of  $A_3 \rightarrow A_3 \times A_3 \rightarrow D_6$  the adjoint of  $D_6$  decomposes as

$$\mathbf{66} = 3 \times \mathbf{15} + \mathbf{1} + \mathbf{20}'. \quad (2.37)$$

The  $D_6$  group can be further embedded in  $D_7$  or  $E_7$  giving a rank one enhancement. In either case, the box representation appears in the decomposition of the adjoint. As discussed further in Section 4, we expect that a further analysis of 6D Weierstrass models for  $A_3$  on a singular curve of arithmetic genus 3 on  $\mathbb{P}^2$  will give a global model with a local singularity type giving matter in the box representation of  $SU(4)$ ; the group theory mechanism just described provides one natural way in which this may occur.

## 3. Systematic analysis of Weierstrass models

We now perform a systematic analysis of Weierstrass models for  $SU(N)$  gauge groups on a general F-theory base. Thus we are looking for an  $A_{N-1}$  ( $I_N$ ) Kodaira type singularity on a codimension one space described by a divisor  $\{\sigma = 0\}$ . We assume in the analysis that  $\{\sigma = 0\}$  is nonsingular, so that any ring of local functions  $R_\sigma$  on a sufficiently small open subset of  $\{\sigma = 0\}$  is a unique factorization domain (UFD). We comment on extensions of this analysis to singular divisors  $\{\sigma = 0\}$  at various points in the discussion.

The idea of this analysis is to use the Kodaira conditions on the form of the singularity to determine the form of the coefficients  $f, g$  in the Weierstrass form for a fairly general

class of models. A related analysis is carried out in [15] using the Tate form for various gauge groups<sup>‡</sup>. Here we primarily use Weierstrass form since the counting of degrees of freedom is clearest in this language. The goal of the analysis here is to follow various branches of the conditions on the discriminant realized by a type  $I_N$  singularity to identify models with matter content associated with various local singularity types such as those identified in the previous section.

We begin with the Weierstrass form

$$y^2 = x^3 + fx + g. \quad (3.1)$$

Here  $f \in -4K$ ,  $g \in -6K$  where  $K$  is the canonical class on the base  $B$ . We expand

$$f = \sum_i f_i \sigma^i, \quad g = \sum_i g_i \sigma^i. \quad (3.2)$$

where as above,  $\{\sigma = 0\}$  is the codimension one locus on the base  $B$  carrying the  $A_{N-1}$  singularity. For this general analysis we leave the dimension of the base and degree of  $\sigma$  unfixed. In the following sections we specialize to the cases where the base is a complex surface (6D space-time theories) or complex 3-fold (4D space-time theories). In most situations we can consider  $f_i, g_i$  as polynomials in local coordinates  $s, t$  (or  $s, t, u$  for 4D theories) on the base, with degrees that will depend on the particular situation. If we are working with an elliptically-fibered Calabi-Yau  $d$ -fold over the base  $\mathbb{P}^{d-1}$ , and the degree of  $\sigma$  is  $b$  then the degrees of  $f_i, g_i$  are

$$[f_i] = 4d - bi, \quad [g_i] = 6d - bi. \quad (3.3)$$

For example, for 6D theories with no tensor multiplets (the case studied from the low-energy point of view in [20]), the dimension is  $d = 3$ , and  $B = \mathbb{P}^2$ , so for an  $SU(N)$  group associated with a singularity on a divisor class of degree  $b = 1$ ,  $f_0$  is a polynomial in  $s$  of degree 12,  $f_1$  has degree 11, etc. Note that since  $f, g$  are really sections of line bundles, they can generally only be treated as functions locally.

The discriminant describing the total singularity locus is

$$\Delta = 4f^3 + 27g^2. \quad (3.4)$$

We can expand the discriminant in powers of  $\sigma$ ,

$$\Delta = \sum_i \Delta_i \sigma^i. \quad (3.5)$$

For an  $I_N$  singularity type we must have  $\Delta_i = 0$  for  $i < N$ . For each power of  $\sigma$ , the condition that  $\Delta_i$  vanish imposes various algebraic conditions on the coefficients  $f_i, g_i$ . These conditions can be derived by a straightforward algebraic analysis (some of which also appears in [15]).

---

<sup>‡</sup>The results of [15] are complementary to the ones derived here, and include the case of  $SU(N)$  for large  $N$ .

For local functions  $\Phi$  and  $\Psi$  defined on an open set of the base  $B$ , we use the notation

$$\Phi \sim \Psi \tag{3.6}$$

to indicate that  $\Phi$  and  $\Psi$  have identical restrictions to  $\{\sigma = 0\}$ , i.e.,  $\Phi|_{\{\sigma=0\}} = \Psi|_{\{\sigma=0\}}$ . Equivalently,  $\Phi$  and  $\Psi$  differ by a multiple of  $\sigma$ , i.e.,  $\Phi = \Psi + \mathcal{O}(\sigma)$ .

We proceed by systematically imposing the condition that the discriminant (3.4) vanish at each order in a fashion compatible with an  $A_{N-1}$  singularity on  $\{\sigma = 0\}$ .

$\Delta_0 = 0$ :

The leading term in  $\Delta$  is

$$\Delta_0 = 4f_0^3 + 27g_0^2. \tag{3.7}$$

For this to vanish in a fashion compatible with an  $A_{N-1}$  singularity, we must be able to locally express  $f_0, g_0$  in terms of some  $\phi$  by

$$\begin{aligned} f_0 &\sim -\frac{1}{48}\phi^2 \\ g_0 &\sim \frac{1}{864}\phi^3 \end{aligned} \tag{3.8}$$

Moreover, when  $N \geq 3$ ,  $\phi$  has a square root (locally), and we can rewrite this condition as

$$\begin{aligned} f_0 &\sim -\frac{1}{48}\phi_0^4 \\ g_0 &\sim \frac{1}{864}\phi_0^6 \end{aligned} \tag{3.9}$$

The condition that  $f_0|_{\{\sigma=0\}} = x^2$  for some  $x \in R_\sigma$  follows from the condition that the ring of local functions on sufficiently small open subsets of the variety defined by  $\{\sigma = 0\}$  is a unique factorization domain (so each factor of  $g_0|_{\{\sigma=0\}}$  must appear an even number of times in  $(f_0|_{\{\sigma=0\}})^3$ ); the local function  $x$  on the divisor  $\{\sigma = 0\}$  can then be “lifted” to a function  $X$  on an open subset of  $B$  such that  $X|_{\{\sigma=0\}} = x$ . Note that the existence of  $X$  is definitely only a local property in general: [15] has an explicit example that shows that it may not be possible to find  $X$  (or its square root when that is appropriate) globally. The condition that  $X$  is itself a square modulo  $\sigma$  follows from the “split” form of the singularity in the Tate algorithm [26, 9] for determining the Kodaira singularity type from the Weierstrass form<sup>§</sup>. This condition can be seen explicitly in the  $A_3$  and  $A_5$  examples described in Sections 2.1 and 2.2. In those cases,  $f_0$  is proportional to  $s^4$ , modulo  $\sigma$ . If  $s^4$  in these situations were replaced with  $s^2$ , the exceptional curve in the first chart would be defined by  $y^2 = sx^2$ , and would not factorize into  $C_1^\pm$ , so that the resulting gauge group would be the symplectic group  $Sp(N)$  instead of  $SU(N)$ . The numerical coefficients in

---

<sup>§</sup>When  $N = 2$ , there is no split form and no monodromy, and we cannot conclude that  $X$  is a square modulo  $\sigma$ .

(3.8) and (3.9) are chosen to simplify parts of the algebra in other places and to match with other papers including [15] <sup>¶</sup>.

We phrase the arguments of this section in terms of quantities such as  $\phi_0$  that are in general only locally defined functions. However, in some key examples (such as the ones at the beginning of Section 4) it is known that these quantities are actually globally defined on  $B$ . In those cases, we are easily able to count parameters in the construction by considering the degrees of these globally defined objects.

$\Delta_1 = 0$ :

In light of (3.8), we now replace  $f_0$  and  $g_0$  by  $-\phi^2/48$  and  $\phi^3/864$ , respectively. This may produce additional contributions to  $f, g$  at higher order in  $\sigma$ , since for example the original  $f_0$  was only equal to  $-\phi^2/48$  up to terms of order  $\sigma$ . Such additional contributions can be absorbed by redefining the coefficients  $f_i$  and  $g_i$  from (3.2) accordingly. The coefficient of the leading term in the discriminant then becomes

$$\Delta_1 = \frac{1}{192} (12\phi^3 g_1 + \phi^4 f_1) . \quad (3.10)$$

This vanishes exactly when

$$g_1 = -\frac{1}{12}\phi f_1 . \quad (3.11)$$

A similar term must be removed from  $g_i$  at each order (this can be seen just from the terms  $g_0 g_i, f_0^2 f_i$  in the discriminant; a more general explanation for this structure is described at the end of this section), so we generally define

$$\tilde{g}_i = g_i + \frac{1}{12}\phi f_i \quad (3.12)$$

$\Delta_2 = 0$ :

After imposing (3.9) (as a substitution) and (3.11), the coefficient of the next term in the discriminant is

$$\Delta_2 = \frac{1}{16} (\phi^3 \tilde{g}_2 - \phi^2 f_1^2) . \quad (3.13)$$

At this stage, we also impose the condition  $\phi = \phi_0^2$  to guarantee  $SU(N)$  gauge symmetry, so that the next term in the discriminant becomes

$$\Delta_2 = \frac{1}{16} (\phi_0^6 \tilde{g}_2 - \phi_0^4 f_1^2) . \quad (3.14)$$

For (3.14) to vanish in our UFD,  $f_1|_{\{\sigma=0\}}$  must be divisible by  $\phi_0|_{\{\sigma=0\}}$ , so there is a locally defined function  $\psi_1$  such that

$$f_1 \sim \frac{1}{2}\phi_0 \psi_1 . \quad (3.15)$$

---

<sup>¶</sup>For reference, we give a dictionary relating the variables used here to analogous variables used in [15]. The variables  $(\phi_0, \phi_1, \phi_2, \dots, \psi_1, \psi_2, \dots)$  in this paper correspond to the variables  $(s_0, u_1, u_2, \dots, t_1, t_2, \dots)$  in [15]. Note that  $\mu$  from [15] must be set equal to 1 to match this paper.

We replace  $f_1$  by  $\frac{1}{2}\phi_0\psi_1$  and adjust coefficients accordingly; we can then solve  $\Delta_2 = 0$  for  $\tilde{g}_2$ , obtaining:

$$\tilde{g}_2 = \frac{1}{4}\psi_1^2. \quad (3.16)$$

(Note from (3.12) that this last equation is equivalent to  $g_2 = \frac{1}{4}\psi_1^2 - \frac{1}{12}\phi_0^2 f_2$ .)

**SU(4)** ( $\Delta_3 = 0$ ):

At the next order in  $\sigma$  the coefficient in the discriminant is

$$\Delta_3 = \frac{1}{16} (\phi_0^6 \tilde{g}_3 - \phi_0^3 \psi_1^3 - \phi_0^5 \psi_1 f_2). \quad (3.17)$$

We see that in order for  $\Delta_3$  to vanish along  $\{\sigma = 0\}$ ,  $\psi_1|_{\{\sigma=0\}}$  must be divisible by  $\phi_0|_{\{\sigma=0\}}$ . Thus, there must exist a locally defined function  $\phi_1$  such that

$$\psi_1 \sim -\frac{1}{3}\phi_0\phi_1. \quad (3.18)$$

We replace  $\psi_1$  by  $-\frac{1}{3}\phi_0\phi_1$  and adjust coefficients accordingly; we can then solve  $\Delta_3 = 0$  for  $\tilde{g}_3$ , obtaining:

$$\tilde{g}_3 = -\frac{1}{3}\phi_1 f_2 - \frac{1}{27}\phi_1^3 \quad (3.19)$$

(This last equation is equivalent to  $g_3 = -\frac{1}{12}\phi_0^2 f_3 - \frac{1}{3}\phi_1 f_2 - \frac{1}{27}\phi_1^3$ .) Again, a term such as the first term on the RHS of (3.19) will arise for each  $\tilde{g}_i$ , so we define

$$\hat{g}_i = \tilde{g}_i + \frac{1}{3}\phi_1 f_{i-1} \quad (3.20)$$

and the latter condition (3.19) is just  $\hat{g}_3 = -\phi_1^3/27$ . It is also convenient to define  $\hat{f}_2 = f_2 + \frac{1}{3}\phi_1^2$ .

We have now arranged a theory with an  $SU(4)$  local factor in the gauge group. The construction is completely general, given our assumption about  $\{\sigma = 0\}$  being nonsingular. Making the substitutions above, adjusting coefficients, and expanding  $f, g$ , and  $\Delta$  we have

$$f = -\frac{1}{48}\phi_0^4 - \frac{1}{6}\phi_0^2\phi_1\sigma + f_2\sigma^2 + f_3\sigma^3 + f_4\sigma^4 + \mathcal{O}(\sigma^5) \quad (3.21)$$

$$g = \frac{1}{864}\phi_0^6 + \frac{1}{72}\phi_0^4\phi_1\sigma + \left(\frac{1}{36}\phi_0^2\phi_1^2 - \frac{1}{12}\phi_0^2 f_2\right)\sigma^2 + \left(-\frac{1}{12}\phi_0^2 f_3 - \frac{1}{3}\phi_1 f_2 - \frac{1}{27}\phi_1^3\right)\sigma^3 + g_4\sigma^4 + \mathcal{O}(\sigma^5) \quad (3.22)$$

$$\Delta = \frac{1}{16}\phi_0^4(-\hat{f}_2^2 + \phi_0^2\hat{g}_4)\sigma^4 + \mathcal{O}(\sigma^5) \quad (3.23)$$

We see that at a generic point on the curve  $\{\sigma = 0\}$  the singularity type is  $I_4$ , with vanishing degrees of  $f, g, \Delta$  of 0, 0, 4, corresponding to an  $A_3$  singularity giving a  $SU(4)$  gauge group. At the roots of  $\phi_0$ , the vanishing degrees become 2, 3, 6, corresponding to a  $D_4$  singularity, giving a two-index antisymmetric ( $\Lambda^2$ ) matter representation. The remaining part of the leading component of the discriminant,  $\tilde{\Delta}_4 = \Delta_4/\phi_0^4 = (-\hat{f}_2^2 + \phi_0^2\hat{g}_4)/16$ , is of degree  $8d - 4b$ . For generic choices of the coefficients of the other functions  $\phi_1, f_2, \dots$ , the roots of  $\tilde{\Delta}_4$  will correspond to an enhancement to  $A_4$ , giving matter in the fundamental



representation of  $SU(4)$ . For non-generic choices of the functions  $f_2, \phi_1$ , there can be enhanced singularities. In particular if  $f_2$  and  $\phi_0$  share a root the degree of vanishing of  $f$  is enhanced to 3. The following table shows the possibilities for enhanced singularities

Label	Root	$f$	$g$	$\Delta$	Singularity	G/Rep.
$4_0$	generic	0	0	4	$A_3$	$SU(4)$
$4_a$	$\tilde{\Delta}_4 = 0$	0	0	5	$A_4$	$\square$
$4_b$	$\phi_0 = 0$	2	3	6	$D_4$	$\square (\Lambda^2)$
$4_c$	$\phi_0 = 0, f_2 = 0$	3	3	6	$D_4$	$\square$
$4_d$	$\phi_0 = f_2 = \phi_1 = 0$	3	4	8	$E_6$	$[\square + 2\square]$

The explicit local resolution of singularity type  $4_b$  with  $A_3$  enhancement to  $D_4$  is that described in Section 2.1, with details in Section A.1 of the Appendix. Replacing  $\phi_0 \rightarrow 2s, f_2 \rightarrow -1$ , and for simplicity  $\phi_1 \rightarrow 0$  (which does not affect the singularity),  $f, g$  from (3.21) and (3.22) take precisely the forms (2.2) used in that analysis. In the last case ( $4_d$ ) a more exotic singularity appears but no new matter representations arise. The brackets in the table indicate that we have not explicitly resolved the singularity, but the matter content is uniquely determined by the 6D anomaly cancellation conditions, as we discuss in the following section.

**SU(5)** ( $\Delta_4 = 0$ ):

The vanishing of the leading term in (3.23) requires that  $\hat{f}_2|_{\{\sigma=0\}}$  be divisible by  $\phi_0|_{\{\sigma=0\}}$ . Thus, in this case there exists a locally defined function  $\psi_2$  such that

$$\hat{f}_2 \sim \frac{1}{2}\phi_0\psi_2. \quad (3.24)$$

We replace  $\hat{f}_2$  by  $\frac{1}{2}\phi_0\psi_2$  and adjust coefficients accordingly; we can then solve  $\Delta_4 = 0$  for  $\hat{g}_4$ , obtaining:

$$\hat{g}_4 = \frac{1}{4}\psi_2^2. \quad (3.25)$$

(In other words,  $f_2$  has been replaced by  $\frac{1}{2}\phi_0\psi_2 - \frac{1}{3}\phi_1^2$  and  $g_4 = \frac{1}{4}\psi_2^2 - \frac{1}{12}\phi_0^2 f_4 - \frac{1}{3}\phi_1 f_3$ .) We have now arranged a theory with an  $SU(5)$  local factor in the gauge group (again completely general, assuming  $\{\sigma = 0\}$  is nonsingular). Expanding  $f, g$ , and  $\Delta$  we have

$$f = -\frac{1}{48}\phi_0^4 - \frac{1}{6}\phi_0^2\phi_1\sigma + \left(\frac{1}{2}\phi_0\psi_2 - \frac{1}{3}\phi_1^2\right)\sigma^2 + f_3\sigma^3 + f_4\sigma^4 + f_5\sigma^5 + \mathcal{O}(\sigma^6) \quad (3.26)$$

$$g = \frac{1}{864}\phi_0^6 + \frac{1}{72}\phi_0^4\phi_1\sigma + \left(\frac{1}{18}\phi_0^2\phi_1^2 - \frac{1}{24}\phi_0^3\psi_2\right)\sigma^2 \quad (3.27)$$

$$+ \left(-\frac{1}{12}\phi_0^2 f_3 - \frac{1}{6}\phi_0\phi_1\psi_2 + \frac{2}{27}\phi_1^3\right)\sigma^3$$

$$+ \left(\frac{1}{4}\psi_2^2 - \frac{1}{12}\phi_0^2 f_4 - \frac{1}{3}\phi_1 f_3\right)\sigma^4 + g_5\sigma^5 + \mathcal{O}(\sigma^6)$$

$$\Delta = \frac{1}{16}\phi_0^4(\phi_0^2\hat{g}_5 - \phi_0\psi_2 f_3 + \phi_1\psi_2^2)\sigma^5 + \mathcal{O}(\sigma^6) \quad (3.28)$$

The range of possible singularities is similar to that encountered in the  $SU(4)$  case above. At the roots of  $\phi_0$  the singularity type is enhanced to  $D_5$ , and the roots of the remaining  $\tilde{\Delta}_4 = \Delta_4/\phi_0^4$  give  $A_5$  singularities. There are also various enhanced singularities for non-generic configurations, but no new matter representations are possible. We again summarize the possible singularity types in the following table

Label	Root	$f$	$g$	$\Delta$	Singularity	G/Rep.
$5_0$	generic	0	0	5	$A_4$	$SU(5)$
$5_a$	$\tilde{\Delta}_4 = 0$	0	0	5	$A_5$	$\square$
$5_b$	$\phi_0 = 0$	2	3	7	$D_5$	$\boxplus (\Lambda^2)$
$5_c$	$\phi_0 = \phi_1 = 0$	3	4	8	$E_6$	$[\boxplus + \square]$
$5_d$	$\phi_0 = \psi_2 = 0$	2	3	8	$D_6$	$[\boxplus + \square]$
$5_e$	$\phi_0 = \phi_1 = \psi_2 = 0$	3	5	9	$E_7$	$[\boxplus + 2\square]$

**SU(6)** ( $\Delta_5 = 0$ ):

The analysis becomes more interesting at the next order. Using the above conditions the leading order term in the discriminant is

$$\Delta_5 = \frac{1}{16}\phi_0^4(\phi_1\psi_2^2 - \phi_0\psi_2f_3 + \phi_0^2\hat{g}_5). \quad (3.29)$$

From this it follows that each root of  $\phi_0|_{\{\sigma=0\}}$  must either divide  $\phi_1|_{\{\sigma=0\}}$  or  $\psi_2|_{\{\sigma=0\}}$ . We can find locally defined functions  $\alpha$  and  $\beta$  such that

$$\phi_0 \sim \alpha\beta, \quad (3.30)$$

where  $\alpha|_{\{\sigma=0\}}$  is the greatest common divisor of  $\phi_0|_{\{\sigma=0\}}$  and  $\psi_2|_{\{\sigma=0\}}$ . There must then also be locally defined functions  $\phi_2$  and  $\nu$  such that

$$\psi_2 \sim -\frac{1}{3}\alpha\phi_2 \quad (3.31)$$

$$\phi_1 \sim \beta\nu. \quad (3.32)$$

Note that by construction,  $\beta|_{\{\sigma=0\}}$  and  $\phi_2|_{\{\sigma=0\}}$  are relatively prime.

We make all of the corresponding substitutions and adjust coefficients; then (3.29) becomes:

$$\Delta_5 = \frac{1}{48}\alpha^6\beta^5 \left( \phi_2(f_3 + \frac{1}{3}\nu\phi_2) + 3\beta\hat{g}_5 \right). \quad (3.33)$$

In order for this to vanish we then must have  $(f_3 + \frac{1}{3}\nu\phi_2)|_{\{\sigma=0\}}$  divisible by  $-3\beta|_{\{\sigma=0\}}$  and  $\hat{g}_5|_{\{\sigma=0\}}$  divisible by  $\phi_2|_{\{\sigma=0\}}$ , with identical quotients. That is, there must exist a locally defined function  $\lambda$  such that

$$f_3 \sim -\frac{1}{3}\nu\phi_2 - 3\beta\lambda \quad (3.34)$$

$$\hat{g}_5 \sim \phi_2\lambda. \quad (3.35)$$

The second relation can also be written as

$$\begin{aligned}
g_5 &\sim -\frac{1}{12}\phi_0^2 f_5 - \frac{1}{3}\phi_1 f_4 + \phi_2 \lambda \\
&\sim -\frac{1}{12}\alpha^2 \beta^2 f_5 - \frac{1}{3}\beta \nu f_4 + \phi_2 \lambda
\end{aligned}
\tag{3.36}$$

The possible singularities are now

Label	Root	$f$	$g$	$\Delta$	Singularity	G/Rep.
$6_0$	generic	0	0	6	$A_5$	$SU(6)$
$6_a$	$\tilde{\Delta}_6 = 0$	0	0	7	$A_6$	$\square$
$6_b$	$\alpha = 0$	2	3	8	$D_6$	$\boxplus (\Lambda^2)$
$6_c$	$\beta = 0$	3	4	8	$E_6$	$\frac{1}{2} \boxplus (\Lambda^3)$
$6_d$	$\alpha = \beta = 0$	3	5	9	$E_7$	$[\frac{1}{2} \boxplus + \square]$
$6_e$	$\beta = \nu = 0$	4	4	8	$E_6$	$[\frac{1}{2} \boxplus]$
$6_f$	$\alpha = \nu = 0$	3	5	9	$E_7$	$([\frac{1}{2} \boxplus + \square] / \boxplus)$

We see now the appearance of a 3-index antisymmetric matter field. The singularity types  $6_b$  and  $6_c$  are precisely the enhancements of  $A_5$  to  $D_6$  and  $E_6$  analyzed locally in Section 2.2, with details in Section A.2 of the Appendix. To relate (3.26), (3.27) to the local forms there we use (3.30), (3.31) and make the replacements

$$(6_b) : \alpha \rightarrow s, \beta \rightarrow 2, \phi_2 \rightarrow -6, \nu \rightarrow 3/2, \lambda \rightarrow 0, f_4 \rightarrow 0, \tag{3.37}$$

$$(6_c) : \alpha \rightarrow 1, \beta \rightarrow 2s, \phi_2 \rightarrow -6, \nu \rightarrow 3/2, \lambda \rightarrow 0, f_4 \rightarrow 0. \tag{3.38}$$

The replacement (3.38) gives (2.11) with  $\rho = s$ . Thus produces a half-hypermultiplet in the  $\Lambda^3$  representation. Two coincident roots of  $\beta$  give  $\rho = s^2$ , for a full hypermultiplet in the  $\Lambda^3$  representation, as discussed in Section 2.2.

It is interesting to note that the  $6_b$  and  $6_c$  singularities with  $D_6$  and  $E_6$  enhancements are connected. If we consider a  $6_c$  branch with  $\beta = 0$ , we can continuously deform the coefficients of the Weierstrass form so that the root  $\beta$  coincides with a root of  $\phi_2$ . At this point, the root of  $\phi_2$  divides  $\phi_0$ , so in the decomposition (3.30), (3.31) the simultaneous root of  $\beta, \phi_2$  becomes a root of  $\alpha, \nu$ , giving a singularity of type  $6_f$ . The root of  $\alpha$  can then be deformed independently of  $\nu$ . In six dimensions, this deformation transforms a combination of a half hypermultiplet in the  $\Lambda^3$  representation and a hypermultiplet in the fundamental representation into a single hypermultiplet in the  $\Lambda^2$  representation. This novel phase transition is clear from the F-theory description but does not have a simple description in the low-energy theory in terms of Higgsing. We describe an explicit example of a transition of this kind in a specific 6D theory in the following section. Note that the intermediate state in this transition associated with a singularity of type  $6_f$  involves a local

enhancement  $A_5 \subset E_7$  with rank increase of more than one. This kind of transition will be discussed further elsewhere.

**SU(7)** ( $\Delta_6 = 0$ ):

At order 7, it becomes more difficult to identify the general Weierstrass form. Imposing the conditions above, the 6th order term in the discriminant is

$$\Delta_6 = \frac{1}{16}\alpha^4\beta^3 \left[ -\frac{1}{9}\beta(\nu\phi_2 - 9\beta\lambda)^2 + \alpha^2 \left( \frac{1}{27}\phi_2^3 + \frac{1}{3}\beta^2\phi_2f_4 + \beta^3\hat{g}_6 \right) \right] \quad (3.39)$$

We do not have a completely general form for the structure needed to make this term vanish. But there are two special cases in which we can carry out the analysis and guarantee the vanishing of (3.39)

**Case 7A**

$$\beta = 1 \quad (3.40)$$

$$\lambda = \frac{1}{9}\nu\phi_2 - \frac{1}{6}\psi_3\alpha \quad (3.41)$$

$$\hat{g}_6 = -\frac{1}{27}\phi_2^3 + \frac{1}{4}\psi_3^2 - \frac{1}{3}\phi_2f_4. \quad (3.42)$$

In this case the local singularities can appear as in the following table

Label	Root	$f$	$g$	$\Delta$	Singularity	G/Rep.
$7_0$	generic	0	0	7	$A_6$	$SU(7)$
$7_a$	$\tilde{\Delta}_7 = 0$	0	0	8	$A_7$	$\square$
$7_b$	$\alpha = 0$	2	3	9	$D_7$	$\square (\Lambda^2)$
$7_c$	$\alpha = \nu = 0$	4	6	12	$\star$	$\Delta T$

In case  $7_c$  the singularity of degrees 4, 6, 12 goes outside the Kodaira list. To resolve the singularity, the codimension two singularity locus on the base must be blown up. In six-dimensional gravity theories this leads to the appearance of an additional tensor multiplet.

**Case 7B**

In general, for (3.39) to vanish we must have  $(\alpha|_{\{\sigma=0\}})^2$  divisible by  $\beta|_{\{\sigma=0\}}$ . We can then write

$$\beta \sim \gamma\delta^2 \quad (3.43)$$

for appropriate locally defined functions  $\gamma$  and  $\delta$  such that  $(\gamma\delta)|_{\{\sigma=0\}}$  is the GCD of  $\alpha|_{\{\sigma=0\}}$  and  $\beta|_{\{\sigma=0\}}$ . We must then have  $\alpha|_{\{\sigma=0\}}$  divisible by  $(\gamma|_{\{\sigma=0\}})^2$  and furthermore we can decompose

$$\alpha \sim \gamma^2\delta\xi \quad (3.44)$$

$$\nu \sim \gamma\zeta. \quad (3.45)$$

for appropriate locally defined functions  $\xi$  and  $\zeta$ . We can arrange for (3.39) to vanish (case B) if we make the assumption that  $\gamma = \xi = 1$ , so that  $\beta \sim \alpha^2$ . In this case the singularities that can arise are

Label	Root	$f$	$g$	$\Delta$	Singularity	G/Rep.
$7'_0$	generic	0	0	7	$A_6$	$SU(7)$
$7'_a$	$\tilde{\Delta}_7 = 0$	0	0	8	$A_7$	$\square$
$7'_b$	$\alpha = \beta = 0$	3	5	9	$E_7$	$\left[ \begin{array}{c} \square \\ \square \end{array} (\Lambda^3) \right]$
$7'_c$	$\alpha = \nu = 0$	4	6	13	$\star$	$\Delta T$

The singularities at  $\alpha = \beta$  give rise to 3-index antisymmetric matter representations of  $SU(7)$ .

### SU(8) and beyond

A complete treatment of all possible branches of the Weierstrass model for  $A_7$  and beyond would be very involved algebraically. We do not attempt a complete analysis but describe the generic structure of Weierstrass models giving codimension one  $A_{N-1}$  singularities for  $N \geq 8$ . To proceed further we need to get  $\Delta_7$  to vanish. This cannot be done in case B above since vanishing at order 8 given the conditions imposed in that case would give a common root to  $\beta$  and  $\phi_2$ , which is not possible since  $\beta$  and  $\phi_2$  are relatively prime. We can, however proceed to arbitrary order in  $N$  under the generic assumption that  $\beta = 1$ . This corresponds to case 7A above. Note that all of the representations beyond the fundamental and  $\Lambda^2$  representations arose from situations where  $\beta \neq 1$ .

First, we note that the condition  $\beta = 1$  simplifies the algebra at  $SU(6)$  and beyond. This condition sets  $\alpha = \phi_0$  and replaces (3.31) with

$$\psi_2 \sim -\frac{1}{3}\phi_0\phi_2, \quad (3.46)$$

and fixes  $\nu = \phi_1$ . Furthermore, (3.34) and (3.41) become

$$f_3 \sim \frac{1}{2}\phi_0\psi_3 - \frac{2}{3}\phi_1\phi_2. \quad (3.47)$$

We can proceed with the generic  $A_{N-1}$  model by simply following this pattern. To get an  $SU(8)$  model we substitute

$$\psi_3 \sim -\frac{1}{3}\phi_0\phi_3, \quad (3.48)$$

and solve for  $g_7$ . To get an  $SU(9)$  model we substitute

$$f_4 \sim \frac{1}{2}\phi_0\psi_4 - \frac{2}{3}\phi_1\phi_3 - \frac{1}{3}\phi_2^2, \quad (3.49)$$

and solve for  $g_8$ . To get an  $SU(10)$  model we substitute

$$\psi_4 \sim -\frac{1}{3}\phi_0\phi_4, \quad (3.50)$$

and solve for  $g_9$ , etc.

A simple way of expressing the conditions being imposed is that the leading terms in the expansions of  $f, g$  can be written in the form

$$f = -\frac{1}{3}\Phi^2 + \mathcal{O}(\sigma^k) \quad (3.51)$$

$$g + \frac{1}{3}\Phi f = -\frac{1}{27}\Phi^3 + \mathcal{O}(\sigma^{2k}) \quad (3.52)$$

for  $SU(2k)$ , and

$$f = -\frac{1}{3}\Phi^2 + \frac{1}{2}\sigma^k\phi_0\psi_k + \mathcal{O}(\sigma^{k+1}) \quad (3.53)$$

$$g + \frac{1}{3}\Phi f = -\frac{1}{27}\Phi^3 + \frac{1}{4}\sigma^{2k}\psi_k^2 + \mathcal{O}(\sigma^{2k+1}) \quad (3.54)$$

for  $SU(2k+1)$ , where

$$\Phi = \frac{1}{4}\phi_0^2 + \phi_1\sigma + \phi_2\sigma^2 + \phi_3\sigma^3 + \cdots + \phi_{k-1}\sigma^{k-1}. \quad (3.55)$$

(This is the same form used in the inductive argument given in [15] for  $SU(N)$  with large  $N$ .)

In this way, we can find a systematic solution out to the point where there are no more  $g_i$ 's for which to solve. In the following section we describe the details of how the analysis continues beyond this point for a specific class of 6D models.

The numerical factors here, and the form of the equation, can be explained by converting our Weierstrass equation (3.1) to Tate form. Let  $\Upsilon = \phi_1 + \phi_2\sigma + \phi_3\sigma^2 + \cdots + \phi_{k-1}\sigma^{k-2}$ , so that  $\Phi = \frac{1}{4}\phi_0^2 + \sigma\Upsilon$ . For  $SU(2k)$ , we convert to Tate form using the coordinate change

$$x = X + \frac{1}{3}\Phi \quad (3.56)$$

$$y = Y + \frac{1}{2}\phi_0 X \quad (3.57)$$

giving an equation of the form

$$Y^2 + \phi_0 XY = X^3 + \sigma\Upsilon X^2 + \sigma^k FX + \sigma^{2k} G. \quad (3.58)$$

Similarly, for  $SU(2k+1)$ , we convert to Tate form using the coordinate change

$$x = X + \frac{1}{3}\Phi \quad (3.59)$$

$$y = Y + \frac{1}{2}\phi_0 X + \frac{1}{2}\sigma^k \psi_k \quad (3.60)$$

giving an equation of the form

$$Y^2 + \phi_0 XY + \sigma^k \psi_k Y = X^3 + \sigma\Upsilon X^2 + \sigma^{k+1} FX + \sigma^{2k+1} G. \quad (3.61)$$

## 4. 6D supergravity without tensor fields

We now use the general analysis of the previous section to describe a particular class of 6D supergravity theories arising from F-theory. We consider the class of 6D models with no tensor multiplets ( $T = 0$ ) and a gauge group having a nonabelian local factor  $SU(N)$ . These theories correspond to F-theory constructions on the base  $\mathbb{P}^2$ .

In [20] theories of this kind were analyzed from the point of view of the anomaly cancellation conditions in the low-energy theory. A complete list of all possible matter representations for each local gauge group factor  $SU(N)$  was constructed for theories with  $T = 0$ . From the point of view of the low-energy theory, each local  $SU(N)$  factor is associated with an integer  $b \in \mathbb{Z}_+$  appearing in the anomaly polynomial and topological  $BF^2$  couplings of the theory. For theories with an F-theory realization,  $b$  is the degree of the divisor on  $\mathbb{P}^2$  carrying the  $SU(N)$  local factor. For small values of  $b$ , anomaly analysis of the 6D supergravity theories shows that  $N$  can range up to 24, and the set of possible matter representations is strongly constrained. For larger values of  $b$  the range of possible values of  $N$  is more restricted, but a wider range of possible matter representations is compatible with the anomaly conditions. We now recall from [20] the possible matter content for models with gauge group  $SU(N)$  and small values of  $b$ , and consider the explicit F-theory constructions of such models.

### 4.1 $SU(N)$ on curves of degree $b = 1$

From anomaly cancellation alone, the complete set of possible matter representations for an  $SU(N)$  local factor with  $b = 1$  in a 6D  $\mathcal{N} = 1$  supergravity theory is constrained to the following combinations of matter fields (note that for  $N = 3$  the antisymmetric  $\Lambda^2$  representation is really the (conjugate of) the fundamental representation while for  $N = 2$  the fields denoted by this representation are really uncharged.):

$b = 1$   $SU(N)$  matter possibilities

$N$	$\square$	$\boxplus$	$\boxminus$	neutral
$N \leq 24$	$24 - N$	3	0	$273 - N(45 - N)/2 - 1$
6	$18 + k$	$3 - k$	$k/2, k \leq 3$	$155 - k$
7	22	0	1	132

We now show that global F-theory models can be realized for theories with  $SU(N)$  gauge group and all these possible matter representations through the general construction described in the previous section, except the special cases  $N = 21, 23$ . Furthermore, the number of neutral scalar fields in each of these models can be identified with the number of unfixed parameters in the Weierstrass description of each model when  $N < 18$ .

For  $b = 1$  on  $\mathbb{P}^2$ , the structure of the general Weierstrass model is fairly simple. Taking the locus of the  $SU(N)$  to be the zero locus of the function  $\sigma = t$  (in appropriate local coordinates  $s, t$  on  $\mathbb{P}^2$ ), the functions  $f_i, i = 0, \dots, 12$  in the expansion of  $f$  (3.2) are polynomials in  $s$  of degree  $12 - i$ , and the functions  $g_i, i = 0, \dots, 18$  are polynomials in  $s$

of degree  $18 - i$ . The functions  $f_i$  contain  $1, \dots, 13$  coefficients for a total of 91 coefficients while the  $g_i$  contain 190 coefficients. The total number of coefficients appearing in the Weierstrass polynomials  $f, g$  is therefore 281. There is a redundancy in this description under general linear transformations of homogeneous coordinates  $s, t, u$  on the F-theory base  $\mathbb{P}^2$ , removing 9 parameters. The total number of independent parameters in the Weierstrass model is therefore  $281 - 9 = 272$ . There is one further scalar appearing in the low-energy 6D theory associated with the overall Kähler modulus of the base, so the number of scalar fields associated with the Weierstrass moduli is in precise agreement with the gravitational anomaly condition, which states that

$$H - V = 273, \tag{4.1}$$

where  $H, V$  are the numbers of charged matter hypermultiplets and vector multiplets in the generic model.

Now we apply the methods of Section 3. Since  $\{\sigma = 0\}$  is a line in  $\mathbb{P}^2$ , all of the functions  $\phi_0, \phi_1, \dots$ , etc. that occur in the analysis are in fact homogeneous polynomials on  $\mathbb{P}^2$  whose degrees are easily determined<sup>||</sup>. Fixing the first few orders of the discriminant to vanish, (3.9) fixes the  $13 + 19 = 32$  coefficients in  $f_0, g_0$  in terms of the four coefficients of  $\phi_0$ , thus removing 28 coefficients. When the singularity locus is fixed at  $t = 0$  this removes two of the redundancies in the linear transformation parameters. Fixing  $\Delta_1 = 0$  through (3.11) removes another 18 degrees of freedom by fixing  $g_1$  in terms of  $\phi_0, f_1$ , leaving  $272 - 46 + 2 = 228$  degrees of freedom in the Weierstrass coefficients<sup>\*\*</sup>. Fixing  $\Delta_2 = 0$  through (3.15) and (3.16) removes another 20, bringing the number of unfixed parameters in the  $SU(3)$  model to 208. This corresponds precisely to the number of scalar fields (209) in the  $N = 3$  model from the table above. Fixing  $\Delta_3 = 0$  through (3.17) removes another 19 parameters, leaving 189 degrees of freedom in the Weierstrass coefficients, again in agreement with the 190 expected scalar fields for the  $SU(4)$  model above. Note that the degrees of freedom in the Weierstrass coefficients are complex degrees of freedom, while the hypermultiplets parameterize a quaternionic Kähler moduli space and hence contain four real scalars. There are thus additional real degrees of freedom not captured by the Weierstrass coefficients; these are associated with degrees of freedom on the branes [34], and may be related to the T-brane construction of [35].

We now consider in more detail the matter content in the set of theories with  $SU(4)$  gauge group. The 189 complex-dimensional moduli space of Weierstrass models with  $SU(4)$  realized on a curve on  $\mathbb{P}^2$  of degree  $b = 1$  describes a family of generic models with 3 matter fields in the two-index antisymmetric ( $\Lambda^2$ ) representation. This set of F-theory

---

<sup>||</sup>For curves of higher degree, particularly ones of higher genus, this statement may fail to hold and the global analysis is more subtle.

<sup>\*\*</sup>Note that the count we are performing here only applies to  $SU(N)$ ,  $N \geq 3$ , since the Weierstrass coefficients for  $SU(2)$  involve  $\phi$  rather than  $\phi_0$ . In the case of  $SU(2)$ , we use (3.8) to fix the 32 coefficients in  $f_0, g_0$  in terms of the seven coefficients of  $\phi$ , removing only 25 coefficients this time; (3.11) still removes another 18 degrees of freedom, leaving 231 degrees of freedom in the Weierstrass coefficients. The “extra” 3 degrees of freedom are accounted for by the fact that the  $\Lambda^2$  representation is trivial, so the three copies of  $\Lambda^2$  provide 3 additional neutral fields. We thank Volker Braun for discussion on this point.



models satisfies the conditions (3.9-3.23), and for a generic model in this class there are three distinct roots of  $\phi_0$  giving singularity type  $4_b$ . For each such root, we can choose a local coordinate  $s$  so that  $s = 0$  at the root, and we can expand

$$\phi_0 = 2s + \mathcal{O}(s^2). \quad (4.2)$$

Plugging (4.2) into (3.21), (3.22), and choosing  $\phi_1 = 0, f_2 = -1$  gives precisely the expressions (2.2) for  $f, g$  used in the  $A_3 \rightarrow D_4$  singularity analysis of Section 2.1. For any  $\phi_1, f_2$  an equivalent analysis will give a local singularity enhancement from  $A_3$  to  $D_4$  giving matter in the two-index antisymmetric ( $\Lambda^2$ ) representation. Thus, these models all have 3 matter fields in the  $\Lambda^2$  representation, in agreement with the generic class of models identified from the anomaly analysis. The discriminant locus  $\Delta$  is divisible by  $\phi_0^4$ , and the remaining factor  $\tilde{\Delta}_4$  is a degree 20 polynomial in  $s$  and has 20 roots associated with singularities of type  $4_a$  providing 20 fundamental representations, and completing the matter content of these theories. Though various non-generic singularities can be constructed by tuning some roots of the discriminant to coincide, such as the  $E_6$  type singularity realized when  $\phi_0 = \phi_1 = f_2 = 0$ , the anomaly analysis guarantees that such singularities cannot change the total matter content of the theory as long as the gauge group remains  $SU(4)$  and no singularity becomes bad enough to provide an extra tensor multiplet.

Continuing to higher  $N$ , the top class of models in the table above is associated with generic singularities at the vanishing locus of  $\phi_0$ , with no additional singularity structures. As  $N$  increases up to  $N = 17$ , at each step an additional  $3+20-N$  degrees of freedom in the Weierstrass form are fixed, matching the decrease in uncharged scalar degrees of freedom in the low-energy theory. For small  $N$  more restricted classes of Weierstrass coefficients reproduce the other models in the table.

For  $SU(5)$  the story is very similar to  $SU(4)$ . There is a 171-dimensional space of models with 3  $\Lambda^2$  matter hypermultiplets and 19 hypermultiplets in the fundamental representation.

For  $SU(6)$  the most generic model has  $\phi_0 = \alpha$ , so there are three singularities of type  $6_b$  giving  $\Lambda^2$  representations and 18 fundamentals. In this case, however, there are now other possibilities. Up to 3 of the roots of  $\phi_0$  can be in  $\beta$ , corresponding to singularities of type  $6_c$ , and giving half-hypermultiplets in the  $\Lambda^3$  representation. This precisely reproduces the range of possible  $SU(6)$  models in the table above. There are several interesting features of these models. First, consider the number of unfixed Weierstrass degrees of freedom in these configurations. From (3.31), (3.32) we see that the number of degrees of freedom in  $\psi_2, \phi_1$  is reduced by 3 when fixing the  $A_5$  singularity, independent of the distribution of roots between  $\alpha$  and  $\beta$ . From (3.34), however, we see that the number of degrees of freedom in  $f_3$  (*i.e.*, in  $\lambda$ ) is reduced by one for each root of  $\beta$ . Therefore, the dimension of the space of models with  $k$  roots  $\beta = 0$  is reduced by  $k$  from that of the generic  $SU(6)$  moduli space. This agrees with the numbers of neutral scalar fields listed in the table above for these models. When  $\beta = s$ , as discussed in Section 2.2, the  $E_6$  singularity is incompletely resolved, giving a half-hypermultiplet in the  $\Lambda^3$  representation. When two roots of  $\beta$  coincide, however, we have  $\beta = s^2$ , giving a full  $\Lambda^3$  hypermultiplet.

A further interesting feature of the  $SU(6)$  models is the possibility of a continuous phase transition between models with different numbers of  $\Lambda^3$  representations. Consider a model with a (half-hypermultiplet)  $\Lambda^3$  representation associated with a type  $6_c$  singularity at a root  $r$  of  $\beta = 0$ . Such a model will also have an  $A_6$  at every root of  $\phi_2$ . By tuning one parameter, a root of  $\phi_2$  and the root  $r$  of  $\beta$  can be made to coincide. But at this point, this is a common root of  $\phi_0$  and  $\psi_2$ , and therefore from the definitions of  $\alpha$  and  $\beta$  becomes a root of  $\alpha$  and  $\nu$ , and also of  $\lambda$ , with  $\alpha$  and  $\lambda$  increasing in degree by one and  $\beta$  decreasing in degree by one. At this point there is a singularity of type  $6_f$ , as discussed in Section 3. From here, however, the roots of  $\alpha$ ,  $\lambda$  and  $\nu$  can be freely and independently varied. This phase transition thus has the effect of transforming matter between the representations

$$\frac{1}{2} \begin{array}{|c|} \hline \square \\ \hline \square \\ \hline \end{array} + \square \rightarrow \begin{array}{|c|} \hline \square \\ \hline \end{array}. \quad (4.3)$$

This is not a simple Higgsing transition, since the gauge group does not change. There is no obstruction to such a transition from anomalies, since the anomaly content of the matter representations is the same on both sides of the transition. We leave a further study of this type of continuous F-theory transition between different types of matter for further work.

For  $SU(7)$ , we again have a generic class of models of the correct dimension with three  $\Lambda^3$  representations. There is also a model of type 7B discussed in the previous section. Since  $\phi_0$  has 3 roots, in the decomposition (3.43),  $\alpha, \beta, \gamma, \delta$  can have respectively 1, 2, 0, 1 roots. There is a single singularity of type  $7'_b$  in such models, associated with a single  $\Lambda^3$  representation.

We have thus reproduced all matter possibilities for  $SU(N)$  models with  $b = 1$ . We return to the discussion of the generic class of models for  $N \geq 8$ . As discussed above, by tuning 3 parameters in an  $f_i$  at each step through a relation like (3.49) or (3.50), and  $20 - N$  parameters through  $g_{N-1}$ , we can continue to generate  $A_{N-1}$  singularities up to a certain point. This continues up to  $SU(17)$  without change, generating models with these groups having three  $\Lambda^3$  matter representations and the correct number of degrees of freedom. The story changes slightly, however, at  $SU(18)$ . At this point, the equation analogous to (3.50) would be  $\psi_8 = -\frac{1}{3}\phi_0\phi_8$ , imposing the condition that  $\psi_8$  vanishes wherever  $\phi_0$  vanishes. Since  $\psi_8$  is linear, however, it must vanish. But  $\psi_8$  only has 2 degrees of freedom, so the correspondence between the number of degrees of freedom in the Weierstrass model and the number of neutral scalar fields breaks down at this point. We return to this point below; nonetheless, we can continue to construct models with  $SU(N)$  groups beyond this point by setting  $\psi_8 = 0$ . The next point where the analysis diverges from the general pattern is at  $SU(20)$ . At this point there is no further function  $g_{19}$  to fix, and  $\psi_9$  is a scalar that we can set to 0. This is enough to guarantee vanishing of the discriminant to order 20. At the next order, fixing  $f_{10}$  to match (3.51) immediately guarantees vanishing to order 22, and fixing  $f_{11}$  in an analogous fashion gives a discriminant of order 24. The correspondence with the number of neutral scalar fields becomes quite unclear in these last steps, since in the 6D theories the number of neutral scalars is expected to *increase* at 24 (with 20 neutral scalars for  $SU(24)$ , 19 for  $SU(23)$  and  $SU(22)$ , and 20 for  $SU(21)$ ).

In any case, we can move directly to the end of the process just described and write a general form for a class of models with  $SU(24)$  local gauge group and three antisymmetric matter representations

$$\begin{aligned}
f &= -\frac{1}{3}\Phi^2 + \tilde{F}_{12}t^{12} \\
g &= -\frac{1}{3}\Phi f - \frac{1}{27}\Phi^3 = \frac{2}{27}\Phi^3 - \frac{1}{3}\Phi\tilde{F}_{12}t^{12} \\
\Phi &= \left[ \frac{1}{4}\phi_0^2 + \phi_1t + \phi_2t^2 + \phi_3t^3 \cdots + \phi_6t^6 \right],
\end{aligned} \tag{4.4}$$

where  $\phi_0$  is a polynomial in  $s$  of degree 3,  $\phi_k$  is a polynomial in  $s$  of degree  $6 - k$  for  $k > 0$  and  $\tilde{F}_{12}$  is a constant (note that  $G$  in (3.58) is set to vanish in this class of models). If  $\tilde{F}_{12}$  is set to 0, then the model becomes everywhere singular.

This is a good opportunity to comment on why our discussion has always been about “local” gauge groups. The geometry of the singular fibers in an elliptic fibration actually determines only the Lie algebra of the gauge theory, and there are typically several different compact Lie groups with the same Lie algebra. (In the mathematics literature, these groups are said to be “locally isomorphic.”) The actual gauge group is determined by the torsion in the Mordell–Weil group of the elliptic fibration [6]. For the  $SU(24)$  example just given, we show below that the Mordell–Weil group is in fact the group  $\mathbb{Z}_2$  with two elements, and this implies that the true gauge group of the theory is  $SU(24)/\mathbb{Z}_2$  rather than  $SU(24)$ .

To see that this local  $SU(24)$  example has a non-trivial Mordell–Weil group, it is convenient to rewrite the example in Tate form, as in (3.58). The result is

$$Y^2 + \phi_0XY = X^3 + t\Upsilon X^2 + t^{12}\tilde{F}_{12}X. \tag{4.5}$$

where  $\Upsilon = \phi_1 + \phi_2t + \phi_3t^2 \cdots + \phi_6t^5$ . The elliptic curve contains the point  $(X, Y) = (0, 0)$  and has a vertical tangent there, for every value of  $s$  and  $t$ . This implies by the usual geometric law of addition on elliptic curves [36] that  $(0, 0)$  is a point of order 2 in the group law on each elliptic curve, so that the corresponding section defines a point of order two in the Mordell–Weil group.

We have thus explicitly reproduced all the (local)  $SU(N)$  models in the table above, except  $SU(23)$  and  $SU(21)$ . It is possible that those two gauge groups can be realized through Higgsing of the  $SU(24)$  model or specialization of models with lower gauge groups. It is also possible that the limitations we have encountered in constructing F-theory models with these groups correspond to physical constraints, perhaps associated with the discrete  $\mathbb{Z}_2$  structure in the  $SU(24)$  theory. Further analyses of these models, as well as a precise understanding of the counting of degrees of freedom for the space of models with large  $N$  are left for future work.

## 4.2 $b = 2$

We now consider the  $T = 0$  6D models with an  $SU(N)$  gauge group and  $b = 2$ . For  $b = 2$  the  $SU(N)$  matter structures allowed by anomaly cancellation are

$b = 2$   $SU(N)$  matter possibilities

$N$	$\square$	$\square$	$\begin{array}{ c } \hline \square \\ \hline \end{array}$	$\begin{array}{ c } \hline \square \\ \hline \square \\ \hline \end{array}$
$N \leq 12$	$48 - 4N$	6	0	0
6	$24 + k$	$6 - k$	$k/2 \leq 3$	0
7	$20 + 5k$	$6 - 3k$	$k \leq 2$	0
8	25	2	1	0
8	$16 + 8k$	$6 - 3k$	0	$k/2 \leq 1$

In this case the analysis is slightly more complicated as we cannot just take  $\sigma = t$  and treat  $f_i, g_i$  as functions of  $s$ , since  $\sigma$  is quadratic in  $s, t$ . We do not attempt to do a complete analysis constructing the most general classes of models, but describe some simple salient features of the models in this case.

The equation of a generic nonsingular degree two curve  $\{\sigma = 0\}$  can be put into the form  $\sigma = t^2 - s$  by choosing coordinates appropriately. We can then do an expansion in  $\sigma$  of the form  $f = f_0 + f_1\sigma + \dots$  where the  $f_i$  are linear in  $t$  and otherwise generic polynomials in  $s$ . Treating the expansions in this way we can systematically carry out the analysis using the method described in the previous section, since the ring of functions on sufficiently small open subsets of  $\{\sigma = 0\}$  is a UFD. This becomes complicated in practice since at each step we must use  $t^2 \rightarrow s$  to bring products of functions back to the canonical form where the coefficients in the  $\sigma$  expansion are linear in  $t$ . In principle, this approach leads to constructions of general models with  $b = 2$ .

A non-generic class of such models is where we take  $\sigma = t^2 - s$  with the  $f_i$  being functions only of  $s$ . This simplifies the analysis of roots; the analysis is essentially as in the  $b = 1$  case but each function such as  $\phi_0$  has twice as many roots when considered on  $\{\sigma = 0\}$ ; for example,  $\phi_0$  has six roots on  $\{\sigma = 0\}$ :  $s = r, t = \pm\sqrt{r}$  for each root  $r$  of  $\phi_0$  considered as a function of  $s$ . This leads to a construction of models precisely analogous to those in the  $b = 1$  case, including the models with six  $\Lambda^2$  representations as well as the cases with  $\Lambda^3$  representations of  $SU(6)$  and  $SU(7)$ . Because this simple class of models is not completely generic the number of parameters is smaller than would be associated with the full moduli space, and not all configurations are possible within this Ansatz. In particular, because the roots of any function in  $s$  are always doubled in  $\{\sigma = 0\}$ , we must get an even number of roots of  $\beta$ , and the number of half-hypermultiplets for  $SU(6)$  in the  $\Lambda^3$  representation is always even. Similarly, for  $SU(7)$  the number of  $\Lambda^3$  representations is even, so we can get the model with 2 such representations but not the model with one. To get the other models with odd numbers of  $SU(6)$  and  $SU(7)$   $\Lambda^3$  representations it is necessary to go beyond this Ansatz.

A more generic class of  $b = 2$  models can be identified following the structure of (4.4).

We can construct a generic local  $SU(12)$  model with six  $\Lambda^3$  representations through

$$\begin{aligned} f &= -\frac{1}{3}\Phi^2 + \tilde{F}_6\sigma^6 \\ g &= -\frac{1}{3}\Phi f - \frac{1}{27}\Phi^3 = \frac{2}{27}\Phi^3 - \frac{1}{3}\Phi\tilde{F}_6\sigma^6 \\ \Phi &= \left[ \frac{1}{4}\phi_0^2 + \phi_1\sigma + \phi_2\sigma^2 + \phi_3\sigma^3 \right], \end{aligned} \tag{4.6}$$

where  $\phi_i$  are in the ring of functions on  $\{\sigma = 0\}$ . As in the  $SU(24)$  case for  $b = 1$ , putting the equation into Tate form

$$Y^2 + \phi_0XY = X^3 + \sigma\Upsilon X^2 + \sigma^6\tilde{F}_6X \tag{4.7}$$

shows that  $(0, 0)$  is a point of order 2 in the Mordell–Weil group, and hence the actual gauge group is  $SU(12)/\mathbb{Z}_2$ . Models with smaller gauge groups can be found by adding higher order terms to  $f, g$ , to reduce the order of vanishing of  $\Delta$ . By tuning parameters in such models it should be possible to identify the  $b = 2$  models with odd numbers of (half/full)  $\Lambda^3$  hypermultiplets.

We have not identified the class of global F-theory models giving rise to the  $\Lambda^4$  representation of  $SU(8)$ . As discussed in Section 2, such matter representations should arise from a singularity with a specific  $A_7 \rightarrow E_8$  embedding. Because the  $SU(8)$  model with a single  $\Lambda^4$  representation (i.e.,  $k = 2$  in the last line of the table above) does not contain any  $\Lambda^2$  representations, it seems that this model cannot arise from a complete enhancement to  $E_8$  through the embedding discussed in Section 2. A related mechanism may be at work, however, perhaps involving an incompletely resolved singularity. We leave the identification of the global  $b = 2$  model with this matter structure for further work. We note, however, that since the  $\Lambda^4$  representation of  $SU(8)$  is quaternionic it can come in  $1/2$  hypermultiplet representations. A half hypermultiplet of  $\Lambda^4$  combined with eight fundamental representations has the same contribution to the anomalies as 3  $\Lambda^2$  representations. We thus expect that there may be another class of exotic transitions transforming matter in an  $SU(8)$  gauge group from

$$\frac{1}{2} \begin{array}{|c|} \hline \square \\ \hline \square \\ \hline \square \\ \hline \end{array} + 8 \times \square \rightarrow 3 \times \square. \tag{4.8}$$

Finally, we identify another new type of phase transition associated with  $b = 2$  models. Consider a class of  $b = 2$  models with

$$\sigma = t^2 - \epsilon s, \tag{4.9}$$

where  $\epsilon$  is a parameter for the models. We can use the method described above where each  $f_i, g_i$  is a function purely of  $s$  to construct a subclass of the generic set of models with 6  $\Lambda^3$  representations of  $SU(N)$ . Now we take the parameter  $\epsilon \rightarrow 0$ . This is just a parameter in the space of Weierstrass models. In the limit  $\epsilon = 0$  this becomes a model with a codimension one  $A_{2N-1}$  singularity localized on the zeros of the function  $\sigma' = t$ . This is therefore identical to a  $b = 1$  model with 3  $\Lambda^2$  representations of  $SU(2N)$ . Considered

in the opposite direction, this transition provides a non-standard breaking of an  $SU(2N)$  theory with 3  $\Lambda^2$  representations to an  $SU(N)$  theory with 6  $\Lambda^2$  representations. A related transition has recently been identified in the context of intersecting brane models [37]. We leave a more complete discussion of this type of phase transition for future work.

### 4.3 $b = 3$

For  $b = 3$  the total genus (2.24) associated with the matter content must be 1. The only representations with genus 1 are the adjoint and two-index symmetric ( $\text{Sym}^2$ ) representations. So each model must have one or the other of these. We list the set of possible matter contents for an  $SU(N)$  theory with  $b = 3$

$b = 3$   $SU(N)$  matter possibilities

$N$	$\square$	$\square$	$\begin{array}{ c } \hline \square \\ \hline \square \\ \hline \end{array}$	Adj	$\square\square$
$N \leq 8$	$72 - 9N$	9	0	1	0
$N \leq 8$	$72 - 9N$	10	0	0	1
6	$18 + k$	$9 - k$	$k/2 \leq 4$	1	0
6	$18 + k$	$10 - k$	$k/2 \leq 5$	0	1
7	$9 + 5k$	$9 - 3k$	$k \leq 3$	1	0
7	$9 + 5k$	$10 - 3k$	$k \leq 2$	0	1
8	9	5	1	1	0
8	9	6	1	0	1
9	5	4	1	1	0

Note that the general pattern is that for  $N > 5$ , any number of  $\Lambda^3$  representations can be realized along with  $(N - 4)(N - 3)/2 - 1$  extra fundamentals, at the cost of  $N - 4$   $\Lambda^2$  representations, beginning with the model with 9  $\Lambda^2$ 's, one adjoint, and  $72 - 9N$  fundamentals (or the same with 10  $\Lambda^2$ 's and one symmetric representation instead of the adjoint). Such exchanges are possible in the space of allowed theories except when ruled out by the gravitational anomaly bound on scalar degrees of freedom or positivity of the number of fundamentals; for example at  $SU(9)$  the number of fundamentals would become negative if we attempted to remove the  $\Lambda^3$  representation. As in the  $SU(6)$  case discussed above, we expect that all of these changes in matter can be realized through phase transitions along continuous one-parameter families of F-theory models.

From the anomaly point of view, we can also exchange an adjoint representation, along with one neutral scalar, for one symmetric and one antisymmetric representation. This cannot be done through continuous phase transitions, however, since as discussed in Section 2 the distinction between these representations is determined by global monodromy on the brane structure. Note that there are two models appearing in the list of models with an adjoint that have no corresponding model with an  $\text{Sym}^2$  representation, the model with  $SU(7), k = 3$  and that with  $SU(9)$ . In both cases this can be seen from counting degrees of freedom. These two models with the adjoint representation have a total of  $273 + N^2 - 1$  charged hypermultiplets. Thus there are no uncharged scalars in these models, by (4.1).

To exchange an adjoint for a symmetric and an antisymmetric would require one additional charged hypermultiplet, for a total of  $273 + N^2$ , violating the gravitational anomaly bound.

As in the  $b = 2$  case, we can proceed in several ways to construct models of the generic  $b = 3$  type with 9  $\Lambda^2$  representations and one adjoint. Choosing a generic cubic smooth  $\sigma$ , the corresponding curve is an elliptic curve of genus one, giving one adjoint representation. We can expand order by order in the ring of local functions on  $\{\sigma = 0\}$ , or we can take a cubic such as  $\sigma = t^3 + s$  with non-generic coefficient functions depending only on  $s$ , or we can construct the  $N = 8$  model using an analogous construction to (4.4), (4.6). By continuously deforming  $\sigma$  we can get a singular curve with an equation such as  $\sigma = t^3 + st$  with a double point singularity. Because this is continuously connected to the family of theories with smooth  $\sigma$ , however, this class of models should always have an adjoint representation and not a symmetric representation. We can describe various models with  $\Lambda^3$  matter content as discussed in the  $b = 2$  case above, though as in that discussion we cannot explicitly identify all such models. Note in particular that the single  $N = 9$  model cannot be realized in this way, and must require some further tuning of the Weierstrass coefficients. We leave a further study of these models to future work.

#### 4.4 $b = 4$

Now let us consider degree 4 curves, corresponding to  $b = 4$  matter content in the low-energy theory. For  $b = 4$ , the total genus is 3. So we expect 3 adjoints for a smooth degree 4 curve in F-theory. From the genus formula (2.16), the other possibilities for saturating the genus are either a linear combination of  $3 - x$  adjoints and  $x \text{Sym}^2$  representations for arbitrary  $SU(N)$ , or several exotic possibilities: a single “box” ( $\boxplus$ ) representation for  $SU(4)$  or a  $\boxplus^2$  representation for  $SU(5)$ ; each have genus 3.

There are a variety of anomaly-free low-energy  $SU(N)$  models with various types of matter content, as in the cases with smaller  $b$ . For  $N \leq 6$  there are models with 3 adjoints, 12  $\Lambda^2$  representations, and no  $\Lambda^3$  representations. These correspond to the generic branch in the Weierstrass models as described above and can be constructed in a similar fashion to  $b = 2, 3$ . There are a variety of models that exchange  $\Lambda^2$ 's for  $\Lambda^3$ 's + fundamentals. We assume that these models correspond to various singular limits in a similar fashion to that described above. There are also various models that replace some or all of the adjoints with  $\Lambda^2 + \text{Sym}^2$  (again at the cost of a single neutral scalar). We do not have anything to say about these models that goes beyond the discussion of the analogous models with  $b = 3$ .

The most novel feature that arises at  $b = 4$  is the possibility of a new matter representation as mentioned above. Although there is no apparently-consistent low-energy model that contains the  $\boxplus^2$  representation of  $SU(5)$  at  $b = 4$  (this representation does appear for  $SU(5)$  in combination with 3 adjoints at  $b = 5$ ), for  $N = 4$  there is a model

$$SU(4) : \quad \text{matter} = 1 \times \boxplus + 64 \times \square \quad (4.10)$$

While we identified a group-theoretic embedding of the box representation of  $SU(4)$  in Section 2, we do not have an explicit realization of a theory containing this representation

as a global Weierstrass model on  $\mathbb{P}^2$ . Finding such a singularity may involve an incomplete resolution of some kind, since the embedding  $A_3 \rightarrow D_6$  discussed in Section 2 would otherwise seem to give rise to additional adjoint matter fields. We leave the construction of a global theory describing the model with matter content (4.10) as a challenge for future work.

## 5. 4D models

The general formalism developed for describing  $SU(N)$  models in Section 3 applies just as well to F-theory on an elliptically fibered Calabi-Yau 4-fold as in the case of elliptically fibered threefolds. This provides a framework for systematically analyzing F-theory constructions of 4D theories of supergravity coupled to  $SU(N)$  gauge theories. For 4D F-theory constructions the full story is more complicated, since fluxes must be present [38, 39]. The fluxes generate a superpotential, and nonperturbative contributions from instantons are also present. These effects produce a potential on the moduli space that lifts the continuous flat moduli space to a landscape with separated vacua and stabilized moduli. Nonetheless, underlying this more complicated physics is the continuous moduli space of degrees of freedom associated with the Weierstrass coefficients in an F-theory construction. When the compactification space is large, these moduli will be light, and the moduli space is approximate.

### 5.1 4D Weierstrass models

We do not go far into the issues regarding moduli stabilization and fluxes on 4D F-theory vacua here. F-theory methods for analyzing matter in 4D theories in the presence of flux were developed in [24, 25]; following these works there has been a great deal of recent work on 4D F-theory constructions with particular focus on phenomenological applications (see for example [40, 41, 42, 43]); for reviews of some recent developments in these directions see [4, 44, 45]. In this paper we take a simplistic approach where we ignore fluxes and the lifting of moduli, and consider the tuning necessary in Weierstrass models to achieve an  $SU(N)$  gauge group. We can then consider constructions with matter fields in different representations. Although the number of fields appearing in a particular representation may depend upon the details of fluxes and the full F-theory construction, the type of representation should depend only on the classification of codimension two singularities, on which we are focused here.

In four dimensions, as in six dimensions, the simplest F-theory compactification we may consider is compactification on projective space. We thus consider F-theory on a 4-fold that is elliptically fibered over  $\mathbb{P}^3$ . We consider some explicit examples of the structure of Weierstrass models giving  $\mathcal{N} = 1$  4D supergravity theories in this context. Previous work in which F-theory constructions over  $\mathbb{P}^3$  were considered includes [46].

On  $B = \mathbb{P}^3$  we have  $K = -4H$ , where  $H$  is the hypersurface divisor generating  $H_2(B, \mathbb{Z})$ . The Weierstrass functions  $f, g$  are then polynomials of degree 16 and 24 in local variables  $r, s, t$ , and the discriminant is of degree 48. We are looking for an  $SU(N)$  gauge



group associated with an  $A_{N-1}$  singularity. We consider the discriminant locus on a degree  $b$  hypersurface  $\{\sigma = 0\}$ . The coefficient functions  $f_i(g_i)$  then have degree  $16 - bi, 24 - bi$

We begin as in 6D with  $b = 1$ . We again follow the systematic analysis of Section 3, using  $\sigma = t$ , so that  $f, g$  are functions of  $r, s$ . The function  $\phi_0$  controlling the leading term  $f_0$  is now of degree 4. We can construct generic models with  $SU(N)$  gauge groups by tuning the coefficients to make each term  $\Delta_n$  in the discriminant vanish order by order, as in Section 3. In the generic model, matter will be associated with the points where  $\Delta_N$  acquires extra degrees of vanishing, associated with codimension two singularities. The intersection between  $\{\sigma = 0\}$  and  $\{\phi_0 = 0\}$  defines a curve in  $\mathbb{P}^3$  that is generically a genus 3 curve. There will be matter in the 2-index antisymmetric  $\Lambda^2$  representation of  $SU(N)$  localized on this curve. As mentioned above, a precise determination of the number of matter fields in this representation depends on details of the theory such as fluxes that we do not consider here. The rest of  $\Delta$  defines another divisor (possibly reducible) whose intersection with  $\{\sigma = 0\}$  gives another curve (possibly disconnected) that supports matter in the fundamental representation. Although the curve  $\{\phi_0 = \sigma = 0\}$  is of higher genus, at generic points along this curve the singularity is a codimension two singularity identical to the  $A_{n-1} \rightarrow D_n$  singularities discussed earlier.

The generic 4D model with  $b = 1$  having largest gauge group can be described in a fashion similar to (4.4)

$$\begin{aligned} f &= -\frac{1}{3}\Phi^2 + \tilde{F}_{16}t^{16} \\ g &= -\frac{1}{3}\Phi f - \frac{1}{27}\Phi^3 = \frac{2}{27}\Phi^3 - \frac{1}{3}\Phi\tilde{F}_{16}t^{16} \\ \Phi &= \left[ \frac{1}{4}\phi_0^2 + \phi_1 t + \phi_2 t^2 + \phi_3 t^3 \cdots + \phi_8 t^8 \right], \end{aligned} \tag{5.1}$$

where  $\phi_0$  is a polynomial in  $r, s$  of degree 0,  $\phi_k$  is a polynomial in  $r, s$  of degree  $8 - k$  for  $k > 0$  and  $\tilde{F}_{16}$  is a constant. Once again, we can write this in Tate form

$$Y^2 + \phi_0 XY = X^3 + tYX^2 + t^{16}\tilde{F}_{16}X. \tag{5.2}$$

to see that  $(0, 0)$  is a point of order 2 in the Mordell–Weil group of the elliptic fibration. Thus, the gauge group in this case is  $SU(32)/\mathbb{Z}_2$ . The curve supporting the  $\Lambda^2$  matter is the intersection between  $\{\sigma = 0\}$  and  $\{\phi_0 = 0\}$ . Models with smaller gauge group can be found by adding high-order terms to  $f, g$  to reduce the order of vanishing of the discriminant  $\Delta$ .

Just as in 6D, the parameters of the theory can be tuned so that there are more elaborate codimension two singularities in the 4D  $SU(N)$  models. For an  $SU(6)$  model, for example, as in (3.30), if  $\phi_0$  does not divide  $\psi_2$ , then there must be a component  $\beta$  of  $\phi_0$  that is a factor of  $\phi_1$ . The intersection of  $\{\beta = 0\}$  with  $\{\sigma = 0\}$  gives a curve supporting matter in the  $\Lambda^3$  representation of  $SU(N)$ . Since  $\{\sigma = 0\}$  is smooth, and  $\Delta$  is smooth at generic points, for  $b = 1$  the only general classes of codimension two singularity types are the same as those that can arise for  $b = 1$  models in 4D, namely  $n$ -index antisymmetric matter fields. As we discuss further in the following subsection, this gives a constraint

(though relatively mild) on certain classes of 4D  $\mathcal{N} = 1$  supergravity theories that can be realized in F-theory.

For higher  $b$ , the story is again parallel to that in 6D, although our understanding of the details such as the number of types of each matter field is not as complete without a careful treatment of fluxes. Nonetheless, just as in 6D, matter with a nonzero genus contribution  $g_R$  can only arise when  $b > 2$ , and will be associated with codimension one singularities on  $\{\sigma = 0\}$ .

## 5.2 A (mild) constraint on 4D supergravity theories

The above analysis leads to a constraint on the set of 4D  $\mathcal{N} = 1$  supergravity theories that can be realized from F-theory. This constraint is rather specific to the models associated with the  $\mathbb{P}^3$  compactification, but serves as an example of a constraint on possible low-energy 4D supergravity models.

From the point of view of the 4D theory, the constraint is of the form “any theory with property  $X$  has features  $Y$ ,” where  $X$  describes a set of properties that uniquely determine the F-theory construction to come from an elliptic fibration over  $\mathbb{P}^3$  with a gauge group  $SU(N)$  realized on a divisor  $\{\sigma = 0\}$  of degree  $b = 1$ , and  $Y$  are the constraints on models of this type.

We briefly summarize the features ( $X$ ) of a 4D model that uniquely determine the F-theory base and  $SU(N)$  divisor class to be  $\mathbb{P}^3$  and  $\{\sigma = 0\} = H$ .

We begin with the correspondence between discrete structures in the 4D supergravity theory and in the base of the F-theory compactification; the connection between the F-theory geometry and the low-energy theory is systematically described in [47], and further analysis of this correspondence will appear in [48]. Similar to the story in 6D, a 4D F-theory compactification on a base  $B$  gives rise to topological terms in the low-energy action of the form

$$\begin{aligned}\tau_R &\sim -K \cdot \chi \operatorname{tr} R \wedge R \\ \tau_F &\sim b \cdot \chi \operatorname{tr} F \wedge F,\end{aligned}\tag{5.3}$$

where  $\chi$  are axions coming from wrapping the  $C_4$  Ramond-Ramond field on divisors of the base. In 6D, the corresponding terms appear with two-form fields in place of axions, since  $C_4$  is wrapped on 2-cycles instead of 4-cycles. The  $\tau_F$  term is simply the usual coupling between  $C_4$  and 3-branes associated with instantons on the 7-branes, where  $b$  is the divisor class of the 7-branes carrying the local factor of the gauge group. The  $\tau_R$  term comes from the coupling of the 7-branes to curvature, summed over all 7-branes as described in the 6D case by Sadvov [29], and  $K$  is the canonical class of the base. The number of axions of this type is given by the Hodge number  $h^{(1,1)}(B)$  of the F-theory base. For  $\mathbb{P}^3$ ,  $h^{1,1} = 1$  and there is only one such axion. In general,  $K, b$  are elements of a lattice  $L$ , where the shift symmetries of the axions live in the dual lattice  $L^*$ . In the case of only one axion  $\chi$  such as for F-theory on  $\mathbb{P}^3$ , the couplings in  $\tau_R, \tau_F$  are each quantized so that  $K, b$  are integers.

Now let us consider the special features of the base  $\mathbb{P}^3$  that may be visible in the 4D supergravity theory. There are a number of spaces with  $h^{1,1} = 1$  that could act as bases for

a 4D F-theory compactification. Any such space must be Fano, since  $-K$  must be effective (though note that F-theory bases with  $h^{1,1} > 1$  need not be Fano). Fano spaces with  $h^{1,1} = 1$  have been completely classified [49]. For such a space, the *index* is the ratio  $-K/x$  where  $x$  is the smallest effective divisor class, the generator of  $H^2(B, \mathbb{Z})$ . For projective space  $\mathbb{P}^3$ , the index is 4, since  $K = -4H$ . All other Fano spaces with  $h^{1,1} = 1$  have a smaller value of the index. The ratio between the integers parameterizing the topological couplings (5.3) is the ratio  $-K/b$  between the canonical class of the base and the divisor class characterizing each local factor of the gauge group. This ratio must be less than the index of the F-theory base, since  $b \geq 1$ . Thus, for theories with  $h^{1,1} = 1$ , the maximum value of  $-K/b$  possible is 4, and this value is only attained when the base is  $\mathbb{P}^3$  and the local factor of the gauge group is wrapped on the divisor  $H$ , corresponding to the case  $b = 1$  analyzed above.

Thus, we can state a weak constraint on 4D supergravity theories that come from F-theory: any 4D  $\mathcal{N} = 1$  supergravity theory with only one of the appropriate type of axion, and couplings (5.3) with a ratio of integers  $-K/b = 4$  that has an  $SU(N)$  local gauge group factor must have  $N \leq 32$ , and can only have matter in  $k$ -index antisymmetric representations of  $SU(N)$ . In particular, such a theory cannot have matter in the adjoint representation of the gauge group.

This is not a strong constraint. And there are a number of rather subtle issues in making this constraint rigorous. In particular, the lifting of the moduli by the flux and nonperturbative superpotential make the determination of the spectrum and terms in the action less clear than in 6D theories where the spectrum must be massless. Nonetheless, at least for large volume compactifications the structure of the theory determined by F-theory should be apparent in the low-energy theory, and at least in this regime this constraint should hold.

Despite the limitations in the range of applicability and interpretation of this constraint, it is interesting to study the constraints that F-theory places on 4D supergravity theories. It should not be surprising that such constraints exist; string constructions generally place many constraints on which possible low-energy theories can be realized. In six dimensions, anomalies provide a window on the strong constraints imposed by F-theory constructions [16]-[20], and other F-theory constraints can also be identified as consistency conditions from the point of view of the low-energy theory [21]. Further discussion of constraints on 4D theories from F-theory will appear in [48]. It will be interesting to investigate whether the type of constraint on gauge group and matter content identified in this paper can be generalized and understood in terms of macroscopic consistency conditions from the point of view of 4D supergravity.

## 6. Conclusions

We have explored the structure of some codimension two singularities in F-theory and the matter representations to which they give rise. The focus here has been on understanding how such codimension two singularities arise in global F-theory models. We have developed a very general characterization of global Weierstrass models giving rise to  $SU(N)$  gauge

groups, and analyzed how this general framework applies for F-theory constructions on the bases  $\mathbb{P}^2$  and  $\mathbb{P}^3$ .

It is clear that there is still much unexplored territory in the full range of codimension two singularities. Beyond the standard rank one enhancement studied by Katz and Vafa, there are singularities with incomplete resolution, higher rank enhancement, and singularities associated with singular curves in the base, all of which can give rise to different kinds of matter in F-theory constructions. Further exploring this range of possibilities should provide a fruitful enterprise for further understanding the rôle of matter in F-theory and string theory.

One interesting feature that we have encountered here is the presence of novel phase transitions in F-theory. We have identified phase transitions in which a matter field transforming in the 3-index antisymmetric representation of  $SU(6)$  combines with a matter field in the fundamental representation to produce a matter field in the 2-index antisymmetric representation. This transition does not change the gauge group and hence is not a standard Higgsing transition, but should have some description in the low-energy field theory. There are analogous transitions for the 3-index antisymmetric representation of any  $SU(N)$ ,  $N \geq 6$ . We expect similar transitions for other recombinations of matter fields that leave the 6D anomaly contributions unchanged, such as transitions involving the 4-index representation of  $SU(N)$ ,  $N \geq 8$ . We have also found unusual transitions where the group  $SU(2N)$  breaks to  $SU(N)$  with three matter fields in the two-index antisymmetric representation going to six such fields in the  $SU(N)$  theory. We hope to return to a more detailed study of these exotic phase transitions in future work.

Using global F-theory models on the base  $\mathbb{P}^2$  to describe 6D supergravity theories without tensor multiplets, we have shown that a systematic parameterization of Weierstrass models precisely matches the space of theories identified through anomaly constraints in the low-energy theory, at least for  $SU(N)$  gauge groups supported on curves of low degree in the F-theory base. The structure of matter representations in these theories and number of degrees of freedom matches neatly between F-theory and the low-energy analysis for small  $N$  and degree, with more complicated phenomena arising at higher  $N$  and degree that pose interesting questions for future work.

Applying the global analysis of Weierstrass models to 4D F-theory constructions we have characterized the matter content of a simple class of  $SU(N)$  models on  $\mathbb{P}^3$ . This leads to a mild constraint on 4D supergravity theories, limiting the gauge group and matter content for this specific class of models. This class of models can be identified from the spectrum and topological couplings of the 4D theory. Further work in this direction promises to expand our understanding of F-theory constraints on 4D supergravity theories, and to clarify the structure of matter fields in general F-theory constructions.

## Appendix

### A. Details of singularity resolutions

In this appendix we give detailed analyses of the singularity resolution of various codimen-

sion two singularities described in the main text. We proceed by considering the blow-ups in a sequence of local charts. Note that in these analyses we choose a minimal set of charts to resolve the singularities. In analyzing any given situation, it is generally necessary to check all charts for additional singularities to be sure of a complete resolution.

### A.1 Enhancement of $A_3$ on a smooth divisor class

As a first example we consider the Weierstrass model for the codimension two singularity enhancement  $A_3 \rightarrow D_4$ . As discussed in the main text, after a change of variables a particular form of the local Weierstrass equation for a singularity enhancement of this type is

$$\Phi = -y^2 + x^3 + s^2x^2 - t^2x = 0. \quad (\text{A.1})$$

This is a local equation for the Calabi-Yau threefold described by an elliptic fibration where  $s, t$  are local coordinates on the base  $B$ . At  $t = 0$  there is a codimension one  $A_3$  type singularity that becomes a  $D_4$  singularity on the  $s = 0$  slice.

#### A.1.1 Resolution of $A_3$

The threefold given by (A.1) is singular along the locus  $t = 0$  at  $x = y = 0$  for all values of  $s$ . This singularity can be resolved using a standard procedure of blowing up the codimension one singularity repeatedly until the space is smooth. We do this by working in a sequence of charts containing the various blow-ups. We go through this process in detail in this case, as all other examples will follow in a similar fashion. In this part of the analysis we fix  $s \neq 0$ . We are thus essentially working on a surface that is a two complex dimensional slice of the full Calabi-Yau threefold.

##### Chart 0:

In the original chart we have coordinates  $(x, y, t)$  (treating  $s$  as a constant), and the equation (A.1) gives a singularity at  $x = y = t = 0$ .

##### Chart 1:

To resolve the singularity in chart 0, we blow up the singular point, replacing the point  $(0, 0, 0)$  with a  $\mathbb{P}^2$  given by the set of limit points described by homogeneous coordinates  $[x, y, t]$  along curves approaching  $(0, 0, 0)$ . We choose a local chart that includes the points  $[x, y, 1]$  by changing coordinates to

$$(x, y, t) = (x_1t_1, y_1t_1, t_1). \quad (\text{A.2})$$

In these coordinates, the local equation (A.1) becomes

$$\Phi = (-y_1^2 + s^2x_1^2 + x_1^3t_1 - t_1x_1)t_1^2 = 0. \quad (\text{A.3})$$

The  $\mathbb{P}^2$  that is added through the blow-up process is known as the *exceptional divisor* associated with the blow-up. Factoring out the overall  $t_1^2$  from (A.3) (*i.e.*, removing two copies of the exceptional divisor), we have the equation for the *proper transform* of the original space

$$\Phi_t = -y_1^2 + s^2x_1^2 + x_1^3t_1 - t_1x_1 = 0. \quad (\text{A.4})$$

This equation describes the Calabi-Yau space in chart 1 after the original singularity at  $(x, y, t) = (0, 0, 0)$  has been blown up. (We use the subscript to denote the coordinate chart used for the blow-up.) The intersection of the space defined through (A.4) with the exceptional divisor at  $t_1 = 0$  gives the exceptional divisor on the Calabi-Yau threefold, which (on the surface associated with the slice at fixed  $s$ ) is generally a curve or set of curves associated with blowing up the point at  $t_1 = 0$ . At  $t_1 = 0$ , (A.4) becomes  $-y_1^2 + s^2 x_1^2 = 0$  or

$$y_1 = \pm s x_1. \quad (\text{A.5})$$

This defines a pair of curves that we call  $C_1^\pm$ . The equation (A.4) still contains a singularity at the point  $(x_1, y_1, t_1) = (0, 0, 0)$ , where the curves  $C_1^\pm$  cross. So we must again blow up the singularity to produce a smooth space.

**Chart 2:**

We replace the singular point in Chart 1 with another exceptional divisor  $\mathbb{P}^2$ , this time using the local coordinates

$$(x_1, y_1, t_1) = (x_2, y_2 x_2, t_2 x_2) = 0. \quad (\text{A.6})$$

After removing two copies of the exceptional divisor  $x_2 = 0$  we get the new local equation

$$\Phi_{tx} = -y_2^2 + s^2 + x_2^2 t_2 - t_2 = 0. \quad (\text{A.7})$$

This gives another exceptional curve  $C_2$  (on the surface at each  $s$ ), associated with the intersection of (A.7) with the exceptional divisor  $x_2 = 0$

$$C_2 = \{(x_2, y_2, t_2) : x_2 = 0, t_2 = s^2 - y_2^2\}. \quad (\text{A.8})$$

In homogeneous coordinates on  $\mathbb{P}^2$ ,  $C_2$  is given by the set of points  $[1, y_2, s^2 - y_2^2]$  Since (A.7) has no further singularities, we have completely resolved the local singularity and have a smooth space in coordinate chart 2.

From the way in which the exceptional curves  $C_1^\pm, C_2$  intersect, we identify the  $A_3$  form of the singularity found by Kodaira. To compute the intersections, we write the equation (A.5) for  $C_1^\pm$  in terms of coordinates in chart 2

$$y_2 x_2 = \pm s x_2 \Rightarrow y_2 = \pm s, \quad (\text{A.9})$$

which combined with  $t_1 = t_2 x_2 = 0$  gives the points  $[1, \pm s, 0]$  in homogeneous coordinates on the  $\mathbb{P}^2$  containing  $C_2$ , showing that  $C_1^\pm$  each intersect  $C_2$  at a single point but do not intersect one another, corresponding to the structure of the  $A_3$  Dynkin diagram.

**A.1.2 Resolution of local  $D_4$  singularity on  $s = 0$  slice**

We now return to the form (A.1) for the elliptic fibration with a  $D_4$  singularity at the point  $s = 0$ .

We begin by confirming that on the slice  $s = 0$  there is indeed a singularity whose resolution is described by a set of curves with  $D_4$  structure. To see this we must resolve the singularity given by

$$\Phi = -y^2 + x^3 - t^2 x = 0. \quad (\text{A.10})$$

Following essentially the same procedure as in the  $A_3$  case, we blow up the singularity at  $(x, y, t) = (0, 0, 0)$  by passing to a chart 1 with

$$(x, y, t) = (xt, yt, t)_1. \quad (\text{A.11})$$

Here and in the following examples we will streamline notation by not explicitly including the subscripts in each chart except when necessary. In chart 1, the equation becomes

$$\Phi_t = -y^2 + x^3t - tx = 0. \quad (\text{A.12})$$

The exceptional divisor  $\delta_1$  at  $t = 0$  is then given by  $y^2 = 0$  so

$$\delta_1 = \{(x, 0, 0)\}. \quad (\text{A.13})$$

There are still singularities at  $t = 0$  when  $x^3 - x = 0$ , so at the points

$$x = 0, \pm 1. \quad (\text{A.14})$$

Blowing up each of these three singularities gives three further curves  $\delta_2^{0,\pm}$ , each of which intersects with  $\delta_1$ , and which do not intersect with each other, giving the familiar  $D_4$  singularity resolution.

### A.1.3 Enhancement $A_3 \subset D_4$

Now, let us go through this analysis more carefully for the full threefold incorporating the coordinate  $s$ . This will enable us to understand how the  $A_3$  structure is embedded in the  $D_4$  exceptional curves, giving an explicit characterization of the resulting matter structure in terms of group theory. We wish then to resolve all singularities in the Calabi-Yau threefold defined by

$$\Phi = -y^2 + x^3 + s^2x^2 - t^2x = 0, \quad (\text{A.15})$$

including  $s$  as a coordinate in the analysis.

#### Chart 1:

At the first stage in analysis, the coordinate  $s$  can be carried along as a spectator variable in passing from chart 0 to chart 1, since the point  $(x, y, t) = (0, 0, 0)$  is singular for all  $s$ . Thus, we use the coordinate change

$$(x, y, t, s) = (xt, yt, t, s)_1. \quad (\text{A.16})$$

In chart 1 the full equation then becomes

$$\Phi_t = -y^2 + s^2x^2 + x^3t - tx = 0. \quad (\text{A.17})$$

We see from this that the exceptional curves  $C_1^\pm$  defined by  $y = \pm sx$  (A.5) indeed collapse at  $s = 0$  to the same curve  $\delta_1$  given by  $y = 0$  (A.13). Singularities arise at  $t = 0$  in (A.17) for all  $s$  at  $x = 0$ , and for  $s = 0$  at  $x = \pm 1$ .

#### Chart 2<sub>0</sub>:

The singularity at  $x = 0$  can again be handled by blowing up at each  $s$ , going to coordinate chart  $2_0$  given by

$$(x, y, t, s)_1 = (x, yx, tx, s)_2, \quad (\text{A.18})$$

where

$$\Phi_{tx} = -y^2 + s^2 + x^2t - t = 0. \quad (\text{A.19})$$

In this chart there is a single new exceptional curve given by  $x = 0, t = s^2 - y^2$ , which for generic  $s$  is the curve  $C_2$  from (A.8), and which for  $s = 0$  is the curve  $\delta_2^0$  given by  $x = 0, t = y^2$ .

**Conifold-type double point singularities at  $x = \pm 1$ :**

The story is a little more interesting at the singular points  $x = \pm 1, s = 0$  of (A.17). For example, shifting the coordinate  $x \rightarrow x + 1$  to place the  $x = 1$  singular point at the origin, (A.17) becomes

$$-y^2 + s^2(x + 1)^2 + tx(x + 1)(x + 2) = 0. \quad (\text{A.20})$$

Near the singular point  $(x, y, t, s) = (0, 0, 0, 0)$  this singularity has the form

$$(s - y)(s + y) + 2tx = 0. \quad (\text{A.21})$$

This is the familiar ordinary double point singularity that appears on conifolds [50], and that has played a fundamental rôle in understanding many aspects of string theory vacua. This singularity can be resolved in two different ways to locally give a smooth Calabi-Yau threefold. The resolution can be done by replacing the singular point with a curve  $\mathbb{P}^1$  either by blowing up  $t = 0, s - y = 0$  or by blowing up  $t = 0, s + y = 0$ . In either case, we get an additional exceptional curve at  $s = 0$  that we can call  $\delta_2^+$ . Now, let us consider how the curves  $C_1^\pm$  relate to  $\delta_2^+$ . After the coordinate shift  $x \rightarrow x + 1$ ,  $C_1^\pm$  are given by

$$y = \pm s(x + 1). \quad (\text{A.22})$$

If we resolve the local singularity with a curve by blowing up  $t = s - y = 0$ , then homogeneous coordinates on the new  $\mathbb{P}^1$  are given by  $[x, s + y]$ . In the limit  $x, y, t, s \rightarrow 0$ , the points  $[x, 2s + sx] \sim [x, 2s]$  will be included for  $C_1^+$ , while the points  $[x, -xs] \sim [1, 0]$  will be included for  $C_1^-$ . This shows that in this case, the proper transform of  $C_1^+$  contains all of  $\delta_2^+$ , while the proper transform of  $C_1^-$  only contains one point in  $\delta_2^+$ . If we make the other choice for blowing up the conifold singularity, then  $C_1^-$  contains  $\delta_2^+$  while  $C_1^+$  does not. A similar analysis holds for the resolution of the singularity at  $x = -1$  in (A.17).

The results of this analysis can be summarized as follows: there are two choices that can be made in blowing up each of the two conifold singularities in the full Calabi-Yau threefold given by the local form of the elliptic fibration (A.1). Parameterizing these choices by  $\tau_+, \tau_- \in \{0, 1\}$  and denoting  $\bar{\tau} = 1 - \tau$ , we have an explicit embedding of  $A_3$  into  $D_4$  through

$$\begin{aligned} C_1^+ &\rightarrow \delta_1 + \tau_+ \delta_2^+ + \tau_- \delta_2^- \\ C_1^- &\rightarrow \delta_1 + \bar{\tau}_+ \delta_2^+ + \bar{\tau}_- \delta_2^- \\ C_2 &\rightarrow \delta_2^0. \end{aligned} \quad (\text{A.23})$$



It is straightforward to check that for any of the four possible choices of combinations of  $\tau_{\pm}$ , the intersection form of  $A_3$  is correctly reproduced by this embedding. For example, for  $\tau_+ = \tau_- = 1$

$$C_1^+ \cdot C_1^- = (\delta_1 + \delta_2^+ + \delta_2^-) \cdot \delta_1 = 0, \quad (\text{A.24})$$

using the fact that  $\delta_1 \cdot \delta_1 = -2$  since  $\delta_1$  is a genus 0 curve. The embedding (A.23) for choice of parameters  $\tau_+ = \bar{\tau}_- = 1$  is depicted in Figure 1.

From this embedding of  $A_3$  into  $D_4$  we can read off the matter content in terms of the representation theory of  $SU(4)$ . Each new genus 0 curve that is added to the threefold at the point  $s = 0$  that does not appear at generic  $s$  represents a matter field whose transformation under the  $A_3$  gauge group is determined by the intersection form with the curves forming the  $A_3$  structure. This is the F-theory version [12] of the way in which shrinking 2-cycles produce charged matter in type II [10] and M-theory [11]. In this case, the curves  $\delta_1, \delta_2^{0,\pm}$  form a basis of simple roots for the  $D_4$  algebra. Thus, the complete set of genus 0 curves at  $s = 0$  corresponds to the set of all roots in  $D_4$ . Since the embedding  $A_3 \subset D_4$  is unique up to isomorphism, this corresponds to the standard Katz-Vafa picture in which the gauge group is enhanced by rank 1, and the matter fields are given by the weights of the adjoint representation of  $D_4$  as they transform under  $A_3$  (leaving out the adjoint of  $A_3$ , which corresponds to the generators of the  $SU(4)$  gauge group itself). As discussed in the main text, this gives a matter field in the two-index antisymmetric representation ( $\square$ , or  $\Lambda^2$ ) of  $SU(4)$ .

## A.2 Enhancement of a local $A_5$ singularity

Now, we consider the enhancement of  $A_5$  by various types of local singularities and the associated matter content.

### A.2.1 Enhancement $A_5 \subset D_6$

We begin with the local equation (2.8)

$$\Phi = -y^2 + x^3 + s^2x^2 + 3x^2t + 3t^3x + 2s^2t^2x + s^2t^4 = 0. \quad (\text{A.25})$$

#### Chart 1:

Blowing up in the  $t$  chart (A.16) gives

$$\Phi_t = -y^2 + x^3t + s^2x^2 + 3x^2t + 3t^2x + 2s^2tx + s^2t^2 = 0. \quad (\text{A.26})$$

The exceptional divisor at  $t = 0$  on the threefold is

$$C_1^{\pm} = \{(x, \pm sx, 0, s)\} \quad (\text{A.27})$$

for generic  $s$ , which degenerates to

$$\delta_1 = \{(x, 0, 0, 0)\} \quad (\text{A.28})$$

at  $s = 0$ . There are singularities in (A.26) at  $(0, 0, 0, s)$  for all  $s$  and an additional singularity at  $(-3, 0, 0, 0)$  at  $s = 0$ .

Dealing with the isolated singularity at  $s = 0, x = -3$  first, we change coordinates  $x \rightarrow x + 3$ , where the local form of the singularity becomes (dropping terms of higher than quadratic order)

$$-y^2 + 9tx - 9t^2 + 9s^2 = (3s - y)(3s + y) + 9t(x - t) = 0 \quad (\text{A.29})$$

There are two possible ways of blowing up this conifold singularity, which we parameterize by  $\tau \in \{0, 1\}$ . In each case we denote the exceptional curve by  $\tilde{\delta}_2$ . For  $\tau = 0$  we blow up the point at the origin into a  $\mathbb{P}^1$  at  $t = 3s - y = 0$ , parameterized by homogeneous coordinates  $[x - t, 3s + y]$ . For  $\tau = 0$  the curves  $C_1^\pm$  intersect  $\tilde{\delta}_2$  at the points

$$C_1^+ \cap \tilde{\delta}_2 = \left\{ \lim_{x, y, t, s \rightarrow 0} [x, sx] \right\} = \{[1, 0]\} \in \tilde{\delta}_2 \quad (\text{A.30})$$

$$C_1^- \cap \tilde{\delta}_2 = \left\{ \lim_{x, y, t, s \rightarrow 0} [x, 6s - sx] \right\} = \{[x, 6s]\} = \tilde{\delta}_2 \quad (\text{A.31})$$

so for  $\tau = 0$  the  $s = 0$  limit of  $C_1^-$  contains all of  $\tilde{\delta}_2$ , while  $C_1^+$ , like  $\delta_1$ , intersects  $\tilde{\delta}_2$  at a single point. A similar analysis for the blow-up at  $t = 3s + y = 0$  denoted by  $\tau = 1$  shows that in this case  $C_1^+$  contains  $\tilde{\delta}_2$ , while  $C_1^-$  intersects at only a point. So, just as in (A.23), we can describe the blow-up through a contribution of  $\tau\tilde{\delta}_2$  to  $C_2^+$  and  $\bar{\tau}\tilde{\delta}_2$  to  $C_2^-$ , where  $\bar{\tau} = 1 - \tau$ .

**Chart 2:**

Blowing up the singularity at  $(0, 0, 0, s)$  in (A.26) in the  $x$  chart gives

$$\Phi_{tx} = -y^2 + x^2t + 3tx(t + 1) + s^2(t + 1)^2 = 0. \quad (\text{A.32})$$

The exceptional divisor at  $x = 0$  on the threefold is

$$C_2^\pm = \{(0, \pm s(t + 1), t, s)\} \quad (\text{A.33})$$

for generic  $s$ , which degenerates to

$$\delta_2 = \{(0, 0, t, 0)\} \quad (\text{A.34})$$

at  $s = 0$ . In this coordinate system, we have

$$C_1^\pm = \{(x, \pm s, 0, s)\}. \quad (\text{A.35})$$

There are singularities in (A.32) at  $(0, 0, -1, s)$  for all  $s$  and an additional singularity at  $(0, 0, 0, 0)$  at  $s = 0$ . The latter singularity is associated with the point  $[1, 0, 0]$  in homogeneous coordinates in the  $\mathbb{P}^2$  at the blown up point. A similar analysis in the  $t$  chart shows an analogous singularity at  $s = 0$  at the point  $[0, 0, 1]$ .

The isolated singularities at  $s = 0$  take the conifold form and can be resolved as above. The singularity at the origin in (A.32) has the form

$$(s + y)(s - y) + 3tx = 0. \quad (\text{A.36})$$

Blowing up a  $\mathbb{P}^1$  at  $t = 0, s = \pm y$  gives a curve  $\hat{\delta}_3$  that contributes to  $C_1^\pm$  and to  $C_2^\mp$ . The singularity at homogeneous coordinates  $[0, 0, 1]$  can be analyzed in the  $t$  chart and gives a curve  $\check{\delta}_3$  that contributes only to  $C_2^\pm$ .

**Chart 3:**

Finally, we can blow up the singularity at  $(0, 0, -1, s)$  in (A.32) by shifting  $t \rightarrow t - 1$  and looking in the  $x$  chart again, which gives

$$\Phi_{txx} = -y^2 + s^2t^2 + 3xt^2 + xt - 3t - 1 = 0. \quad (\text{A.37})$$

The exceptional divisor at  $x = 0$  on the threefold is the single curve

$$C_3 = \{(x, y, 0, s) : y^2 = s^2t^2 - 3t - 1\} \quad (\text{A.38})$$

for generic  $s$ , which degenerates to

$$\delta_3 = \{0, y, ((y^2 + 1)/3, 0)\} \quad (\text{A.39})$$

at  $s = 0$ .

By transforming the equations for each of the relevant curves into each coordinate patch we see that the curves  $\delta_{1,2,3}, \tilde{\delta}_2, \hat{\delta}_3, \check{\delta}_3$  have the correct intersection matrix for  $D_6$ , with nonvanishing intersections

$$\tilde{\delta}_2 \cdot \delta_1 = \delta_1 \cdot \hat{\delta}_3 = \delta_2 \cdot \hat{\delta}_3 = \delta_2 \cdot \check{\delta}_3 = \delta_2 \cdot \delta_3 = 1. \quad (\text{A.40})$$

The curves  $C_{1,2}^\pm, C_3$  similarly give  $A_5$ . The embedding  $A_5 \rightarrow D_6$  depends upon three discrete parameters  $\tau, \hat{\tau}, \tilde{\tau}$  describing the choices for the conifold blow-ups, and is given by

$$\begin{aligned} C_1^+ &\rightarrow \delta_1 + \tau\tilde{\delta}_2 + \hat{\tau}\hat{\delta}_3 \\ C_1^- &\rightarrow \delta_1 + \tilde{\tau}\tilde{\delta}_2 + \tilde{\tau}\hat{\delta}_3 \\ C_2^+ &\rightarrow \delta_2 + \tilde{\tau}\hat{\delta}_3 + \check{\tau}\check{\delta}_3 \\ C_2^- &\rightarrow \delta_2 + \hat{\tau}\hat{\delta}_3 + \tilde{\tau}\check{\delta}_3 \\ C_3 &\rightarrow \delta_3 \end{aligned} \quad (\text{A.41})$$

It is straightforward to confirm that this embedding preserves all inner products as needed.

From the decomposition of the adjoint of  $D_5$ , according to the standard rank one reduction, we get a  $\Lambda^2$  antisymmetric representation of  $SU(6)$ .

**A.2.2 Enhancement  $A_5 \subset E_6$**

We now consider models where  $A_5$  is enhanced to  $E_6$ . We begin with (2.11)

$$\Phi = -y^2 + x^3 + \rho^2x^2 + 3\rho x^2t + 3t^3x + 2\rho t^2x + t^4 = 0. \quad (\text{A.42})$$

As discussed in the main text, in (A.42) the parameter  $\rho$  can be either  $\rho = s$  or  $\rho = s^2$ . As we show below, for  $\rho = s$  the  $E_6$  singularity at  $s = 0$  is not completely resolved in the threefold, while it is in the case  $\rho = s^2$ . Most of the following analysis is independent of

the power of  $s$  appearing in  $\rho$ . We describe the differences in the resolution for different choices of  $\rho$  at the end of the discussion.

**Chart 1:**

Blowing up in the  $t$  chart (A.16) gives

$$\Phi_t = -y^2 + x^3t + \rho^2x^2 + 3\rho x^2t + 3t^2x + 2\rho tx + t^2 = 0. \quad (\text{A.43})$$

The exceptional divisor at  $t = 0$  on the threefold is

$$C_1^\pm = \{(x, \pm\rho x, 0, s)\} \quad (\text{A.44})$$

for generic  $s$ , which degenerates to

$$\epsilon_1 = \{(x, 0, 0, 0)\} \quad (\text{A.45})$$

at  $s = 0$ . There is a singularity in (A.43) at  $(0, 0, 0, s)$  for all  $s$ .

**Chart 2:**

Blowing up in the  $x$  chart (A.18) gives

$$\Phi_{tx} = -y^2 + (\rho + t)^2 + x^2t + 3\rho xt + 3t^2x = 0. \quad (\text{A.46})$$

The exceptional divisor at  $x = 0$  on the threefold is

$$C_2^\pm = \{(0, \pm(\rho + t), t, s)\} \quad (\text{A.47})$$

for generic  $s$ , which degenerates to

$$\epsilon_2^\pm = \{(0, \pm t, t, 0)\} \quad (\text{A.48})$$

at  $s = 0$ . There is a singularity in (A.46) where  $t = -\rho$ , at  $(0, 0, -\rho, s)$  for all  $s$ .

**Chart 3:**

Shifting  $t \rightarrow t - \rho$  and blowing up again in the  $x$  chart (A.18) gives

$$\Phi_{txx} = -y^2 + t^2 - 3\rho t - \rho + xt + 3t^2x = 0. \quad (\text{A.49})$$

The exceptional divisor at  $x = 0$  on the threefold is

$$C_3 = \{(0, y, t, s) : y^2 = t^2 - 3\rho t - \rho\} \quad (\text{A.50})$$

for generic  $s$ , which degenerates to

$$\epsilon_3^\pm = \{(0, \pm t, t, 0)\} \quad (\text{A.51})$$

at  $s = 0$ .

At this point, the structure of the singularity at  $(0, 0, 0, 0)$  in chart 3 depends upon whether  $\rho = s$  or  $\rho = s^2$ . In either case, on the slice  $s = \rho = 0$  (A.49) has a singularity at the origin. If, however,  $\rho = s$ , then in the full space there is no singularity, and no further resolution is necessary. In this case the  $E_6$  singularity is not completely resolved, and the

3 curves  $\epsilon_1, \epsilon_3^\pm$  all intersect at a point. If, on the other hand,  $\rho = s^2$  then we have another conifold type singularity at the origin

$$(is + y)(is - y) + t(x + t). \quad (\text{A.52})$$

Resolving this singularity in either way gives another curve  $\epsilon_4$ , which completes the resolution of  $E_6$ .

As above, the intersections of the various curves can be worked out to give the explicit embedding of  $A_5$ . Note that  $C_2^\pm, \epsilon_2^\pm$  are not visible in chart 3; to see these and their intersections with  $C_3, \epsilon_3^\pm$ , another (*e.g.*,  $t$ ) coordinate patch is needed. In the case of the incompletely resolved  $E_6$  when  $\rho = s$ , the embedding is

$$\begin{aligned} C_1^\pm &\rightarrow \epsilon_1 + \epsilon_3^\pm \\ C_2^\pm &\rightarrow \epsilon_2^\pm \\ C_3 &\rightarrow \epsilon_3^+ + \epsilon_3^- \end{aligned} \quad (\text{A.53})$$

This embedding is depicted graphically in Figure 2.

For  $\rho = s^2$ , the  $E_6$  at  $s = 0$  is completely resolved, and the embedding is

$$\begin{aligned} C_1^\pm &\rightarrow \epsilon_1 + \epsilon_4 + \epsilon_3^\pm \\ C_2^\pm &\rightarrow \epsilon_2^\pm \\ C_3 &\rightarrow \epsilon_3^+ + \epsilon_3^- + \epsilon_4 \end{aligned} \quad (\text{A.54})$$

This embedding is depicted graphically in Figure 3.

In the case  $\rho = s$  the matter content contains a half hypermultiplet in the 3-index antisymmetric  $\Lambda^3$  representation, while for  $\rho = s^2$  there is a full hypermultiplet in this representation, as discussed in the main text.

### A.3 Enhancement of $A_3 \rightarrow A_7$ at an ordinary double point

Now we consider a situation where the curve  $\{\sigma = 0\}$  itself becomes singular. As discussed in Section 2.3.2, in such a situation there will be a matter representation with nonzero genus contribution. We consider the ordinary double point singularity in eq. (2.29)

$$\Phi = -y^2 + x^3 + x^2 - s^2 t^2 x = 0. \quad (\text{A.55})$$

This gives a Calabi-Yau threefold with an  $A_3$  singularity along the lines  $s = 0$  and  $t = 0$  with an enhancement to  $A_7$  at the point  $s = t = 0$ . We can resolve the singularity by first resolving the  $t = 0$  singularity in a sequence of charts 1, 2 identical to those used in A.1.1. In the first chart we have  $C_1^\pm$  as before, which correspond to curves  $\gamma_1^\pm$  in the  $A_7$  resolution. In the second chart, using (A.16) we have

$$\Phi_{tt} = -y^2 + x^3 t^2 + x^2 - s^2 x, \quad (\text{A.56})$$

with exceptional curve

$$C_2 = \{(x, y, 0, s) : y^2 = x^2 - s^2 x\} \quad (\text{A.57})$$

that at  $s = 0$  becomes

$$\gamma_2^\pm = \{(x, \pm x, 0, s)\}. \quad (\text{A.58})$$

**Chart 3:**

Now we blow up the singularity at the origin again using the coordinate transformation

$$(x, y, t, s)_2 = (xs, ys, t, s)_3. \quad (\text{A.59})$$

This gives (dropping the  $x^3$  term that is irrelevant for the analysis)

$$\Phi_{tts} = -y^2 + x^2 - sx. \quad (\text{A.60})$$

This has exceptional curves at  $s = 0$  given by

$$\tilde{C}_1^\pm = \{(x, \pm x, 0, 0)\}, \quad (\text{A.61})$$

which we identify with curves  $\gamma_3^\pm$ .

**Chart 4:**

Blowing up one more time using (A.59) gives

$$\Phi_{ttss} = -y^2 + x^2 - x. \quad (\text{A.62})$$

This defines a nonsingular curve  $y^2 = x^2 - x$ , which we identify as  $\tilde{C}_2 = \gamma_4$ .

Following the coordinate charts and determining the intersections of the various curves we have

$$C_1^\pm \rightarrow \gamma_1^\pm \quad (\text{A.63})$$

$$C_2 \rightarrow \gamma_2^+ + \gamma_2^- + \gamma_3^+ + \gamma_3^- + \gamma_4 \quad (\text{A.64})$$

$$\tilde{C}_1^\pm \rightarrow \gamma_3^\pm \quad (\text{A.65})$$

$$\tilde{C}_2 \rightarrow \gamma_4 \quad (\text{A.66})$$

Depending upon how  $A_3$  is embedded into the  $\tilde{C}$ 's relative to the  $C$ 's, this gives an embedding  $SU(4) \rightarrow SU(4) \times SU(4) \rightarrow SU(8)$  under which the decomposition of the adjoint can include either an extra adjoint field or includes a symmetric ( $\text{Sym}^2$ ) and an antisymmetric ( $\Lambda^2$ ) representation. As illustrated in the main text, if the root of  $A_3$  associated with  $C_1^+$  is also associated with  $\tilde{C}_1^-$  then the representation content is symmetric plus antisymmetric.

**Acknowledgements:** We would like to thank Volker Braun, Antonella Grassi, Thomas Grimm, Sheldon Katz, Vijay Kumar, Joe Marsano, Daniel Park, James Sully, Sakura Schäfer-Nameki, and Cumrun Vafa for helpful discussions. Thanks to the Institute for Physics and Mathematics of the Universe (IPMU) for hospitality during the initial phases of this work. WT would like to thank UCSB and DRM would like to thank MIT for hospitality in the course of this work. This research was supported by the DOE under contract #DE-FC02-94ER40818, by the National Science Foundation under grant DMS-1007414, and by World Premier International Research Center Initiative (WPI Initiative), MEXT, Japan.

## References

- [1] C. Vafa, “Evidence for F-Theory,” Nucl. Phys. B **469**, 403 (1996) [arXiv:hep-th/9602022](#).
- [2] D. R. Morrison and C. Vafa, “Compactifications of F-Theory on Calabi–Yau Threefolds – I,” Nucl. Phys. B **473**, 74 (1996) [arXiv:hep-th/9602114](#).
- [3] D. R. Morrison and C. Vafa, “Compactifications of F-Theory on Calabi–Yau Threefolds – II,” Nucl. Phys. B **476**, 437 (1996) [arXiv:hep-th/9603161](#).
- [4] F. Denef, “Les Houches Lectures on Constructing String Vacua,” [arXiv:0803.1194 \[hep-th\]](#).
- [5] W. Taylor, “TASI Lectures on Supergravity and String Vacua in Various Dimensions,” [arXiv:1104.2051 \[hep-th\]](#).
- [6] P. S. Aspinwall and D. R. Morrison, “Non-simply-connected gauge groups and rational points on elliptic curves,” JHEP **9807**, 012 (1998) [arXiv:hep-th/9805206](#).
- [7] J. de Boer, R. Dijkgraaf, K. Hori, A. Keurentjes, J. Morgan, D. R. Morrison, and S. Sethi, “Triples, fluxes, and strings,” Adv. Theor. Math. Phys. **4** (2001) 995–1186, [arXiv:hep-th/0103170](#).
- [8] K. Kodaira, “On compact analytic surfaces. II, III,” Ann. Math. **77** 563 (1963); Ann. Math. **78** 1 (1963).
- [9] M. Bershadsky, K. A. Intriligator, S. Kachru, D. R. Morrison, V. Sadov and C. Vafa, “Geometric singularities and enhanced gauge symmetries,” Nucl. Phys. B **481**, 215 (1996) [arXiv:hep-th/9605200](#).
- [10] S. Katz, D. R. Morrison, and M. R. Plesser, “Enhanced gauge symmetry in type II string theory,” Nucl. Phys. B **477** (1996) 105–140, [arXiv:hep-th/9601108](#).
- [11] E. Witten, “Phase transitions in  $M$ -theory and  $F$ -theory,” Nucl. Phys. B **471** (1996) 195–216, [arXiv:hep-th/9603150](#).
- [12] S. H. Katz and C. Vafa, “Matter from geometry,” Nucl. Phys. B **497**, 146 (1997) [arXiv:hep-th/9606086](#).
- [13] A. Grassi, D. R. Morrison, “Group representations and the Euler characteristic of elliptically fibered Calabi–Yau threefolds”, J. Algebraic Geom. **12** (2003), 321–356 [arXiv:math/0005196](#).
- [14] A. Grassi and D. R. Morrison, “Anomalies and the Euler characteristic of elliptic Calabi–Yau threefolds,” [arXiv:1109.0042 \[hep-th\]](#).
- [15] S. Katz, D. R. Morrison, S. Schafer-Nameki and J. Sully, “Tate’s algorithm and F-theory,” JHEP **1108**, 094 (2011) [arXiv:1106.3854 \[hep-th\]](#).
- [16] V. Kumar and W. Taylor, “String Universality in Six Dimensions,” [arXiv:0906.0987 \[hep-th\]](#).
- [17] V. Kumar and W. Taylor, “A bound on 6D  $\mathcal{N} = 1$  supergravities,” JHEP **0912**, 050 (2009) [arXiv:0910.1586 \[hep-th\]](#).
- [18] V. Kumar, D. R. Morrison and W. Taylor, “Mapping 6D  $\mathcal{N} = 1$  supergravities to F-theory,” JHEP **1002**, 099 (2010) [arXiv:0911.3393 \[hep-th\]](#).
- [19] V. Kumar, D. R. Morrison and W. Taylor, “Global aspects of the space of 6D  $\mathcal{N} = 1$  supergravities,” JHEP **1011**, 118 (2010) [arXiv:1008.1062 \[hep-th\]](#).

- [20] V. Kumar, D. Park and W. Taylor, “6D supergravity without tensor multiplets,” [arXiv:1011.0726 \[hep-th\]](#).
- [21] N. Seiberg, W. Taylor, “Charge Lattices and Consistency of 6D Supergravity,” [arXiv:1103.0019 \[hep-th\]](#).
- [22] M. Esole and S. T. Yau, “Small resolutions of SU(5)-models in F-theory,” [arXiv:1107.0733 \[hep-th\]](#).
- [23] S. H. Katz and D. Morrison, “Gorenstein threefold singularities with small resolutions via invariant theory for Weyl groups,” *Jour. Alg. Geom.* **1**, 449 (1992).
- [24] R. Donagi, M. Wijnholt, “Model Building with F-Theory,” [arXiv:0802.2969 \[hep-th\]](#).
- [25] C. Beasley, J. J. Heckman, C. Vafa, “GUTs and Exceptional Branes in F-theory - I,” *JHEP* **0901**, 058 (2009). [arXiv:0802.3391 \[hep-th\]](#).
- [26] J. Tate, in: *Modular functions of one variable IV*, Lecture Notes in Math, vol. **476**, Springer-Verlag, Berlin (1975), pp. 33–52.
- [27] R. Donagi and M. Wijnholt, “Gluing Branes, I,” [arXiv:1104.2610 \[hep-th\]](#).
- [28] R. Slansky, “Group Theory for Unified Model Building,” *Phys. Rept.* **79**, 1-128 (1981).
- [29] V. Sadov, “Generalized Green-Schwarz mechanism in F theory,” *Phys. Lett. B* **388**, 45 (1996) [arXiv:hep-th/9606008](#).
- [30] D. Perrin, “Algebraic geometry: an introduction,” Springer, 2008.
- [31] E. B. Dynkin, “Semisimple subalgebras of semisimple Lie algebras,” *AMS Transl. ser. 2*, **6** (1957) 111–244.
- [32] K. Oguiso and T. Shioda, “The Mordell-Weil lattice of a rational elliptic surface,” *Comment. Math. Univ. St. Paul.* **40** (1991) 83–99.
- [33] A. Borel and J. De Siebenthal, “Les sous-groupes fermés de rang maximum des groupes de Lie clos,” *Comment. Math. Helv.* **23** (1949) 200–221.
- [34] M. Bershadsky, A. Johansen, T. Pantev, V. Sadov, “On four-dimensional compactifications of F theory,” *Nucl. Phys.* **B505**, 165-201 (1997). [arXiv:hep-th/9701165](#).
- [35] S. Cecotti, C. Cordova, J. J. Heckman, C. Vafa, “T-Branes and Monodromy,” [arXiv:1010.5780 \[hep-th\]](#).
- [36] J. H. Silverman and J. Tate, “Rational points on elliptic curves,” *Undergraduate Texts in Mathematics*, Springer-Verlag, New York, 1992.
- [37] S. Nagaoka, W. Taylor, *to appear*
- [38] K. Becker, M. Becker, “M theory on eight manifolds,” *Nucl. Phys.* **B477**, 155-167 (1996). [arXiv:hep-th/9605053](#).
- [39] K. Dasgupta, G. Rajesh, S. Sethi, “M theory, orientifolds and G - flux,” *JHEP* **9908**, 023 (1999). [arXiv:hep-th/9908088](#).
- [40] C. Beasley, J. J. Heckman, C. Vafa, “GUTs and Exceptional Branes in F-theory - II: Experimental Predictions,” *JHEP* **0901**, 059 (2009). [arXiv:0806.0102 \[hep-th\]](#).
- [41] J. Marsano, N. Saulina, S. Schafer-Nameki, “F-theory Compactifications for Supersymmetric GUTs,” *JHEP* **0908**, 030 (2009). [arXiv:0904.3932 \[hep-th\]](#).



- [42] R. Blumenhagen, T. W. Grimm, B. Jurke, T. Weigand, “Global F-theory GUTs,” Nucl. Phys. **B829**, 325-369 (2010). [arXiv:0908.1784](#) [[hep-th](#)].
- [43] M. Cvetič, I. Garcia-Etxebarria, J. Halverson, “Global F-theory Models: Instantons and Gauge Dynamics,” JHEP **1101**, 073 (2011). [arXiv:1003.5337](#) [[hep-th](#)].
- [44] J. J. Heckman, “Particle Physics Implications of F-theory,” [arXiv:1001.0577](#) [[hep-th](#)].
- [45] T. Weigand, “Lectures on F-theory compactifications and model building,” Class. Quant. Grav. **27**, 214004 (2010). [arXiv:1009.3497](#) [[hep-th](#)].
- [46] A. Klemm, B. Lian, S. S. Roan, S. -T. Yau, “Calabi-Yau fourfolds for M theory and F theory compactifications,” Nucl. Phys. **B518**, 515-574 (1998). [arXiv:hep-th/9701023](#).
- [47] T. W. Grimm, “The N=1 effective action of F-theory compactifications,” Nucl. Phys. **B845**, 48-92 (2011). [arXiv:1008.4133](#) [[hep-th](#)].
- [48] T. Grimm, W. Taylor, *to appear*
- [49] V. A. Iskovskih, “Fano threefolds. I, II,” Math. USSR Izv. **11** (1977) 485–527; **12** (1978) 469–506.
- [50] P. Candelas and X. C. de la Ossa, “Comments on Conifolds,” Nucl. Phys. B **342**, 246–268 (1990).